C.P. No. 1044

C.P. No. 1044

MINISTRY OF TECHNOLOGY

AERONAUTICAL RESEARCH COUNCIL

CURRENT PAPERS

Wind Tunnel Investigation of Jet Interference for Underwing Installation of High Bypass Ratio Engines

by

D. J. Raney, A. G. Kurn

and

J A. Bagley

Aerodynamics Dept , R A.E. Farnborough

LONDON HER MAJESTY'S STATIONERY OFFICE

1969

PRICE 11*s* 6*d* NET

U.D.C. 533.695.178 : 533.6.08 : 533.6.048.2 : 533.6.071

C.P. No. 1044*
March 1968

WIND TUNNEL INVESTIGATION OF JET INTERFERENCE FOR UNDERWING INSTALLATION OF HIGH BYPASS RATIO ENGINES

by

D. J. Raney
A. G. Kurn
J. A. Bagley

Aerodynamics Dept., R.A.E., Farnborough

SUMMARY

Current design proposals for many swept-winged aircraft have large engines of high bypass ratio with short fan cowls on short pylons under the wing, with the annular fan nozzle close to the wing leading edge. With such an arrangement there may be significant changes in the wing pressure distribution induced by the jet flow, particularly that from the fan. In consequence, the normal method of simulating the engine flow in a wind tunnel model, by using simple open ducts, and no representation of the jet thrust, might not be adequate.

The tests reported here were planned as an initial investigation of jet interference for this type of configuration. Results show that for conventional locations of the nacelle on the wing, representation of the cruising jet thrust has only a small effect upon the wing pressure distribution and then only on the lower surface.

---

*Replaces R.A.E. Technical Report 68049 - A.R.C. 30153.

CONTENTS

1 INTRODUCTION

High bypass engines offer substantial improvements in specific fuel consumption but at some penalty in frontal area per unit thrust. At the same time the large increase in payload capacity offered by projected aircraft has encouraged the development of powerplants with a correspondingly high thrust. In consequence, engines are now under development having a static thrust of 40000-50000 lb and a maximum nacelle diameter approaching 10 ft. Two short-cowled fan engines of this size would provide a practical powerplant for a short range high subsonic transport aircraft, as typified by current design studies for an Airbus. For such designs the ratio of nacelle diameter to local wing chord approaches a value of 0.5. These engines, if installed in the conventional podded underwing position, have to be mounted on short pylons with the annular fan nozzle close to the wing leading edge, a position dictated mainly by ground clearance requirements.

In such a position, the displacement flow around the nacelle and pylon affects the flow over the wing, and the jet flow itself may produce additional interference effects, due to the displacement flow or to entrainment of external air into the jet. The intention of the programme of experiments described in this paper was to assess the likely importance of these additional jet interference effects on the flow over the wing, for configurations broadly representative of current Airbus proposals.

A modern wing design has several design features which might make it more susceptible to jet interference than older wings. The nose shape is very carefully shaped to control the development of supercritical flow and delay the appearance of shock-waves; jet entrainment effects in particular might be expected to cause changes in local flow direction near the aerofoil nose - in effect, superposition of additional camber - which could adversely influence the development of supercritical flow. Secondly, modern aerofoil sections are designed to carry more load on the rear part than older sections, which implies that adverse pressure gradients are steep on both lower and upper surfaces. Any increase in gradients, especially on the lower surface, due to jet flow, could well provoke flow separation, or at least excessive thickening of the boundary layer and consequent loss of lift. Thirdly, a modern swept wing relies on the maintenance of swept isobars to delay the onset of supercritical flow and shock waves. Any change in velocities on the wing due to the jet flow will not be uniform across the span and consequently will reduce the

isobar sweep at some place. If the jet interference increases velocities on the lower surface near mid-chord (where the velocity is already greatest) this in combination with loss of isobar sweep could lead to premature appearance of supercritical flow and shocks.

The present experiments were planned to investigate whether any of these possible sources of interference were in fact sufficiently serious to necessitate representation of the jet flow on wind tunnel models of a complete airbus configuration. For this exploratory work, it seemed adequate to measure pressure distributions on a two-dimensional wing with and without the jet flow. It should be possible to infer results for a wing of moderate sweep-back (say, up to 30°) from such measurements.

By restricting the experiment in this way, it was possible to use a good deal of existing apparatus, and this made it possible to start the work quickly. The tests were made in the period February to July 1967.

2 DETAILS OF EXPERIMENTAL APPARATUS

2.1 The tunnel

The tests were made in the 2 ft × 1½ ft transonic tunnel which is installed in the bypass leg of the 8 ft × 6 ft transonic tunnel, and which already has provision for jet blowing. All four walls of the tunnel are slotted with a total open area ratio of 11%; the slots, with corrugated inserts, can be seen in Fig.1. However, the transonic capability of the tunnel was not used in this experiment.

2.2 The wing

Two existing wing models of span 8 inches and chord 5 inches were used, which were borrowed from the National Physical Laboratory. Because these models were made for testing in a smaller tunnel, they did not span the width of the present tunnel. Experiments made by the Boeing Company[1] had shown satisfactory results from tests on a similar model wing mounted between end-plates, so end-plates of diameter 8 inches were fitted to the present wings.

The pressure holes were distributed across a considerable part of the wing surface, as shown in Fig.2, so it was necessary to traverse the wing across the jet (which was fixed) in order to measure a complete chordwise pressure distribution. The rig constructed to enable this to be done is illustrated in Fig.1: a box framework carrying the wing and end-plates is

cantilevered from the tunnel traversing gear, in a fashion which enables the jet to pass downstream without obstruction.

The choice of aerofoils available for this test was somewhat limited. The first section, here referred to as Wing A, was chosen because it had a pressure distribution near the nose on the upper surface which, it was thought, might be particularly sensitive to jet interference, as explained above. The preliminary experiments with this wing, reported in Ref.2, showed that in fact there was little interference with upper surface pressures, and for most of the work reported here, a second aerofoil (Wing B) was used. This had a more representative lower surface pressure distribution than Wing A, which had a suction peak around 5% chord at the incidences used for these tests.

The ordinates of both sections are tabulated in Table 1, with their N.P.L. designations.

Tests were made over a range of Mach numbers from 0.6 up to 0.74, which is approximately the critical Mach number of the two-dimensional wing, at a chord Reynolds number of 1.0 to 1.1 $\times 10^6$. Transition was fixed by a band of 240-200 grade carborundum* between 5% and 10% of the chord.

The tests were made, for the most part, at a single incidence. This was chosen to give a lift coefficient ($C_L = 0.34$) representative of an airbus configuration, so that the deflection of the jet by the wing pressure field should also be broadly representative. In fact, as noted in section 2.4, the jet thrust coefficient is somewhat higher than full-scale, and the jet deflection is likely to be somewhat less than on the full-scale aircraft.

2.3 The jet tube

As in earlier work on jet and base flows (e.g. Ref.3), the jet tube was mounted from the contraction chamber as shown in Fig.1, and fixed on the centre line of the tunnel. The precise location of the nozzle relative to the wing could be set by adjusting the four support struts which can be seen in the contraction.

A disadvantage of this arrangement is that a thick boundary layer develops along the jet tube. In the preliminary experiments[2], this was measured and found to extend out to about the lower surface of the wing, possibly influencing the pressures measured there. In addition, the influence

*This means that the grains of carborundum passed through a sieve with 0.0030 inch square holes, but were retained in a sieve with 0.0025 inch square holes.

of the annular wake surrounding the jet was obviously acting to reduce the jet influence. A suction system was therefore devised to reduce the boundary layer on the tube as much as possible, and this was used throughout the tests reported here, except where explicitly noted. The development of the suction system is being reported separately.

The design of the jet tube and nozzle is illustrated in Fig.3. The jet tube was constructed from two co-axial tubes, with the inner tube supplying the jet air to the nozzle. The tube boundary layer was sucked through longitudinal slots 0.85 inch long and 0.032 inch wide spaced at intervals of 3° around the circumference just ahead of the nozzle, into the annulus between the two tubes and then back down the jet tube out of the tunnel. The suction slots can be seen in the photographs in Fig.1.

2.4 The nozzle and jet flow

The size of the nozzle relative to the wing was chosen to be representative of a twin engine installation on a 30° swept wing short range transport. The geometry of the nozzle represents a typical engine of bypass ratio 5. The throat area of the annular nozzle is 3.3 times that of the central nozzle. The profile of the nozzle is given in Table 2.

Full-scale values of Mach numbers and velocities of the free stream and jet flows, thrust coefficient and jet pressure could not all be correctly represented. It was considered that the shape of the jet boundary should be correctly reproduced and this implied correctly representing the ratio of jet stagnation pressure H_J to free stream static pressure, p_o. The datum value for jet pressure ratio of $H_J = 2.4\ p_o$ was therefore selected, this being typical of the cruising conditions for engines of this type in a short range transport aircraft designed for high subsonic speed. This jet pressure ratio was maintained over the range of Mach number covered by the experiment, so that the development of the jet was effectively unchanged, although the thrust coefficient decreased with increasing Mach number. This and other jet parameters are shown in Fig.4 and compared with full-scale values.

On the full-scale engine at typical cruise conditions the hot central jet and the cold annular fan jet have roughly the same stagnation pressure, and thus also similar unit momentum flows. These characteristics could therefore be represented by feeding the central and annular nozzles from a common air supply without the necessity of providing screens to provide independent control of the two jet flows.

The tunnel free stream and jet flows were both at approximately ambient stagnation temperature, and at these conditions the fan jet velocity and the velocity difference between jet and free stream then also happened to be closely representative of full-scale cruising conditions. The higher velocity of the hot central jet could not be represented but this was considered to be of little significance: this was confirmed later when tests were made with the central nozzle blocked and no significant change in pressures on the wing was measured (Fig.21). More important perhaps, at the correct jet pressure ratio, the thrust coefficient of each of the two jets was about 50% higher at the standard test condition, $M_o = 0.7$, compared with full-scale values at the higher design Mach number of the aircraft. The jet will therefore be less liable to deform in the wing pressure field than full-scale.

Some tests were also made with the jet replaced by an "equivalent solid body", which was shaped to correspond to the outer edge of the jet without allowing for any expansion immediately downstream of the nozzle, nor for the broadening of the jet due to entrainment from the main stream. This solid body extended well downstream of the wing trailing edge and its final cross-sectional area was equal to the sum of the areas of the annular and the central nozzles. Its dimensions are given in Table 3. Such a body could be thought of as representing a very "stiff" jet - i.e. one not deflected or deformed by the wing pressure field, and thus as the opposite limit to the open nacelle with no jet. (The experimental results, reported in section 6.2.1, do not seem to support this interpretation.)

2.5 The test programme

Fig.5 illustrates the different locations of the nacelle relative to the wing which were tested*. The datum configuration (No.2) is close to that proposed in contemporary design studies for a twin-engined Airbus. The "equivalent solid body" is also shown. Some tests were made with only the annular jet represented, the central jet being blocked by a long cylindrical plug.

The wing pressure distribution in the presence of the jet tube was measured under two sets of conditions, at positive jet thrust and at zero jet thrust with the jet total head set equal to the free stream total head, thus simulating free flow through an open duct nacelle. From these results in

*Tests on Wing A at two other heights are not reported here. Some additional results are reported in Ref.2.

conjunction with the pressure distribution of the wing in isolation, the displacement effect of the jet tube and the separate effect of jet thrust have been determined.

Limited measurements have also been made of the deformation of the jet due to the influence of the wing. A few pressure measurements were made on the surface of the rear nozzle, but these are not reproduced here.

3 JET CHARACTERISTICS

The schlieren photographs (Fig.6) of the jet flow show the contraction of the fan jet over the boat tailing of the gas generator cowl. The flow remains attached effectively over the full length of the cowl, oil flow observations showing only a very small separation at the discontinuity which is produced at the end of the cowl.

Little expansion of the jet is apparent at the datum jet pressure ($H_j = 2.4\ p_o$). However, at this condition the fully expanded Mach number is only 1.2 although some limited measurements of pressure distribution over the gas generator cowl indicated that there is in fact considerable over-expansion within the recurring expansion/compression cycle of the jet. At the higher jet pressure ratio, $H_j = 3\ p_o$, the expansion at the nozzle is clearly visible in the photograph. Schlieren photographs were also taken over a range of Mach number from M = 0.6 to 0.74 at $H_J = 2.4\ p_o$ but these were all virtually identical.

Pitot traverses were made through the jet and the wake from the jet tube. Typical results are shown in Fig.7. As the jet is only slightly above choking conditions, total head losses are small through the oblique shock waves within the jet and the normal shock ahead of the pitot tube.

Points worthy of note are the trough in the total head distribution associated with the wake of the gas generator cowl, and the considerable mixing which has taken place between the annular jet and the wake from the jet tube. The flow appeared to be symmetrical around the annular nozzle, with no identifiable wake from the struts supporting the gas generator cowl.

Because of larger losses within the annular section of the nozzle, the total head of the flow from the annular nozzle is somewhat below that from the central nozzle. Since the outer annular jet will inevitably be the main source of the jet interference on the wing, the jet total head was adjusted upwards to bring the mean value for the annular jet up to the datum

value at the exit plane. Values of jet pressure ratio quoted within this Report therefore refer to the annular jet, corresponding values for the central nozzle being some 10% higher.

4 BOUNDARY LAYER ON THE JET TUBE

Because the jet tube extends right forward into the contraction chamber, a thick boundary layer develops along the tube. This is important because, with the wing installed, it will fill much of the space between the propulsive jet and the wing. This cushion of low energy air will tend to influence the wing pressures in two ways. Firstly there will be the direct effect of the reduced velocity of the "free stream" approaching the lower surface. Secondly the boundary layer can be considered as a diffuse annular jet having a negative thrust. This negative thrust is a large fraction of the total net propulsive thrust, so the "jet interference" of the boundary layer may not be negligible compared with that of the propulsive jet, and it will reduce the effect of the jet. It was therefore desirable to minimise the wake from the jet tube as much as possible, and boundary layer suction was applied to the tube as described in section 2.3 above.

A significant variation in the thickness of the natural boundary layer around the jet tube was found, and is shown in Fig.8. The reason for this was not established but it is presumably due to some small cross-flow in the early stages of development of the boundary layer. No significant variation in the distribution around the tube was observed when the tube was moved slightly, nor after the tube was removed and re-installed.

The boundary layer was thickest at the top and bottom of the tube, and relatively thin on one side; as the wing had to be mounted vertically in the tunnel, it was installed on the side of the tube with the thinner boundary layer.

With a sufficient pressure ratio to choke the suction system the boundary layer was thinned fairly uniformly around the tube, and by restricting the suction to that half of the circumference where the natural boundary layer was thinnest, further thinning was obtained in this region. There seemed little tendency for the difference in boundary layer thickness, which then existed, to even out further downstream. Even at the measuring station six inches downstream of the annular nozzle ($x_j = 5.6\ R_o$) a longitudinal position corresponding approximately to that of the wing trailing edge, and about

12 inches downstream of the suction slots, there was a consistently thinner wake over at least $\pm 40^{\circ}$ of arc when suction was applied over only half the tube circumference. Installing the wing on that side of the jet tube did not affect the result. The full programme of tests were therefore made with this suction arrangement.

The circumferential variation of boundary-layer thickness is shown in Fig.8a. Values of displacement thickness and momentum thickness were derived from traverses at $\Theta = 180^{\circ}$ and 270° and are given in the following table.

	$\Theta = 180^{\circ}$, no suction	$\Theta = 270^{\circ}$, no suction	$\Theta = 270^{\circ}$, with suction over half circumference
Displacement thickness	0.093 inch	0.047 inch	0.016 inch
Momentum thickness	0.060 inch	0.032 inch	0.012 inch

However, even with suction the drag coefficient corresponding to the boundary layer thickness on this side of the tube is several times greater than the full scale drag coefficient for the fan cowl.

Profiles of total head measured across the jet in the absence of the wing at various conditions are illustrated in Fig.9. These traverses were made in a horizontal plane, on the side of the jet where the boundary layer was thinnest; the single traverse illustrated in Fig.7 was made vertically across the jet and there are slight differences between this and the corresponding result in Fig.9.

Comparison of the traverses with jet total head equal to free-stream and those with blown jet shows that mixing has considerably reduced the momentum deficiency in the wake in the latter case; but in both cases the beneficial effect of sucking away part of the tube boundary layer is still apparent. The effective radius of the jet is greater at $M_o = 0.6$ than at $M_o = 0.74$ (reflecting the variation of thrust with Mach number shown in Fig.4). In both cases, the jet radius is greater than the radius of the 'equivalent solid body' because of entrainment from the main stream flow, but the outer part of the profile is closely similar for the jet and the solid body.

Total head contours in the wake from the jet tube, with boundary layer suction applied to the jet tube, and without the wing installed in the tunnel, are shown in Fig.10. Although these contours are not streamlines, the outer

contours give an impression of the local flow direction. They reflect the contraction of the flow around the gas generator cowl. Although mixing between the jet and the wake is accelerated with a positive jet thrust, the 99% total head contour is effectively the same for the datum pressure ratio, $H_J = 2.4\ p_o$, the free flow condition, $H_J = H_o$ and for the equivalent solid body.

The effect of the wing on the jet boundary is referred to in section 6.4.

5 TESTS ON THE WING IN ISOLATION

Pressures measured on Wing A in isolation are shown in Fig.11 and results for Wing B are shown in Fig.12. In each case it appears that a satisfactory two-dimensional pressure distribution has been measured, in spite of the spanwise spread of the pressure-measuring points, so the efficacy of the end-plates is confirmed. The comparison in Fig.11 with unpublished measurements at N.P.L. (where the wing is mounted to span the 20in × 8in tunnel) is quite satisfactory, although the tunnel corrections for the present unorthodox experimental arrangement must be uncertain.

Earlier tests by Kurn[4] have shown that the effective blockage of the jet tube is zero, since it extends well forward of the working section, although there will be a small negative blockage correction behind the nozzle because the developed jet has a smaller cross section area than the tube.

For a wing spanning the tunnel, the standard method of Ref.5 predicts a correction of about $\Delta M_o = 0.01$ at a nominal free stream Mach number of 0.72; applying this correction to the present tests brings them well into line with the N.P.L. results. However, as a correction of this magnitude would only alter by about 2% the incremental pressure coefficients which are the main subject of this experiment, no corrections have been applied to the remainder of the results quoted here.

The main series of tests reported here were made with Wing B, for which pressure distributions are presented in Fig.12 for a range of Mach numbers from 0.6 to 0.74. At the datum incidence, a rooftop back to about 35% chord is maintained on the upper surface, and a shock begins to develop at the end of this plateau at about $M_o = 0.7$. The lower surface distribution, with a minimum pressure at around 40% chord, is typical of current designs for subsonic swept wings, and the sectional lift coefficient of 0.34 at $M_o = 0.7$

falls within the band of cruising conditions for a typical short-range transport aircraft.

6 WING AND NOZZLE IN COMBINATION

The main series of results are presented in this section. As stated earlier the majority of the tests were made with the more representative wing, Wing B, and results refer to this wing unless otherwise stated.

The wing pressure distribution measured in the presence of the jet tube, and illustrated in Figs.13-17, include results for positive thrust and zero thrust. Whilst the main purpose of the experiment was the comparison of these two sets of curves, giving the effect of the jet thrust, the corresponding distributions for the isolated wing are also plotted. The difference between the curves for the isolated wing and those for zero thrust represents the displacement effect of the jet tube. This will be roughly similar to the displacement effect of the full-scale nacelle, although the forward part of the nacelle and the intake flow are not properly represented.

6.1 Pressures on upper surface of wing

Typical results for the pressure distribution on the upper surface in the flow of the jet are presented in Fig.13. The spanwise variation of the pressure distribution is not illustrated, but follows the same trends as on the lower surface, discussed below. The contraction of the jet flow around the gas generator cowl reduces the local incidence of the wing and modifies the effective camber, so causing a reduction in local velocities. On a swept wing this would imply some distortion of the isobar pattern on the upper surface, which could cause the drag rise Mach number to be reduced.

There is effectively no influence of jet pressure ratio on the upper surface distribution. Indeed, the upper surface pressures are virtually unchanged over the full ranges of jet pressure and of wing location relative to the jet tube (see Fig.5) and the same distribution was measured with the "equivalent solid body".

It seems safe to conclude that, for this sort of engine installation, the influence of jet thrust on the upper surface isobar pattern can be neglected. This does not necessarily imply that it will be satisfactory to represent the engines by simple flow nacelles, unless these are designed to represent the inlet flow correctly, (which usually needs some increase in exit area compared with the full scale prototype).

6.2 Pressure distributions on lower surface of the wing

6.2.1 Spanwise variation

Some typical examples of the spanwise variation of pressure measured at particular chordwise positions are shown in Fig.14. These are obtained by traversing the wing past the jet, and it was feared that an undesirable interference from the end-plates of the wing might be encountered. The wing span is only eight inches, and the jet diameter is over two inches, so at the extreme limits of the traverse (±1.8 inches from the centre-line) the jet is quite close to the end-plates. However, even for the pressure holes which are farthest from the centre-line, the spanwise variation appears to be symmetrical about a maximum (or minimum), and it does not seem that there is serious interference from the end-plates. As a further check on this point, the flow over the rear part of the "equivalent solid body" was investigated by oil flow techniques; even at the extreme limits of the traverse there was no sign of cross-flow on the body.

The results shown in Fig.14 indicate that the influence of the jet fades out more quickly in the spanwise direction than the influence of the displacement flow around the nozzle. It is also obvious that at some chordwise positions the jet effect and the displacement flow are additive, whereas at other positions they act in opposite senses.

6.2.2 Chordwise variation

The pressure distribution on the lower surface of the wing in the plane of symmetry of the jet is plotted in Fig.15 for the datum configuration, and for jet locations closer to the wing.

At zero thrust, corresponding to free flow through an open nacelle, pressures are increased over the rear 70% of the chord and reduced only over the front 30%, ahead of the suction peak on the isolated wing. As a result, in the datum configuration, the peak suction is reduced considerably, from $C_p = -0.39$ to -0.26.

With the datum jet pressure ratio ($H_J = 2.4\ p_o$), the peak suction is still not increased above that for the wing alone, but it rises rapidly as the jet is moved closer to the wing. Then a sharp suction peak develops near 25% chord, and a secondary peak is formed near 65% chord.

Results are included in Fig.15 for the condition without boundary layer suction applied to the jet tube. The effect is negligible except near the

suction peak, which, with the thicker wake, is reduced slightly (both with zero and finite thrust) for the datum configuration. There is a larger wake effect with the jet closer to the wing.

Variations of jet pressure ratio were tested with the same nozzle geometry to show the sensitivity of wing pressures to this parameter, and to help in the interpretation of the results (Fig.16). However, it should be emphasized that it is the standard pressure ratio, $H_j = 2.4\ p_o$, which is representative of a nozzle with this geometry: higher jet pressure ratios would be characteristic of engines with lower bypass ratio. Such engines would have smaller diameter, and might not have short fan cowls of the type represented in this test.

The effect of increasing jet pressure is very similar to that of bringing the jet tube closer to the wing: the peak suction is increased and a secondary peak appears further aft.

The pressure distribution measured with the "equivalent solid body" (see Fig.16) in lieu of the jet is very similar to that measured with zero jet thrust, except for somewhat higher suctions over the rear part of the chord. This unexpected result suggests that the "solidity" of the jet, and the extent to which it is distorted by the wing pressure field, are less important than some characteristic of the jet which is *not* represented by the solid body. The most important features of this sort are probably the initial expansion of the jet from the nozzle, and the spreading due to entrainment from the external stream.

The lower surface pressure distributions in the plane of the jet for the other nacelle/wing configurations tested are shown in Fig.17. Configuration No.6 (Fig.17a) is similar to the datum but for the smaller wing incidence, and configuration No.5 (Fig.17b) differs from the datum only in the reduced nacelle overhang.

In the first case, the lower incidence has naturally resulted in an increase in local velocities for the wing alone, and the suction peaks with zero and finite thrust are then also increased substantially.

In the latter case, moving the nacelle back relative to the wing has had the effect of moving further back on the wing the incremental pressures produced by the jet tube and the jet. The maximum increments caused by the nozzle displacement flow and by the jet thrust than happen to fall in the region of

the highest velocities over the wing lower surface. Both these increments are thereby increased, and superimposed upon each other they lift the suction peak to about $C_p = -0.9$ for the standard jet condition. This compares with $C_p = -0.38$ for the datum configuration and $C_p = -0.39$ for the isolated wing. The critical pressure coefficient for unswept isobars at this Mach number is $C^*_p = -0.78$, so the flow is locally supersonic with the blown jet: however there is no evidence of a strong shock wave in the flow. Nevertheless, there is little doubt that such regions of high local velocity on the lower surface should be avoided, and these tests with jet thrust represented reinforce the conclusion drawn from earlier tests with open duct nacelles (e.g. Refs.6 and 7) that underwing nacelles should be mounted as far forward as possible.

Fig.18 shows measurements of lower surface pressures (from Ref.2) in the plane of the jet for Wing A. The trends are similar to those discussed above for Wing B. One noteworthy point brought out in these results is that the shape of the pressure distribution, both for zero thrust and for $H_J = 2.4\ p_o$, is essentially similar over a range of Mach numbers, although at $M_o = 0.6$ the flow is entirely subsonic and at $M_o = 0.74$ the peak suction significantly exceeds the local critical value. As in Fig.17, there is no evidence of a strong shock in this case.

6.3 Incremental pressures caused by jet thrust

ΔC_{pJ}, the pressure increment on the wing caused by jet blowing is the change in pressure between finite and zero thrust conditions, viz:-

$$\Delta C_{pJ} = C_{p(H_J)} - C_{p(H_o)}$$

It is this increment that is not represented when tunnel experiments are made with open duct model nacelles.

This lower surface jet interference is plotted in Fig.19 for the four vertical separations of the jet from the wing (configurations 1 to 4). For the datum configuration it is not large, nowhere exceeding ±0.1.

The interference curve is characterised by the suction increment centred around 25% chord and a secondary suction increment in the region near 65% chord. There is also a positive pressure increment in the immediate vicinity of the leading edge. This is of little significance however because of the steep pressure gradient in this region (see Fig.15) and because the velocities here are already low.

There are areas both of positive and negative pressure increment, so the change in sectional lift coefficient due to jet blowing is small: a reduction of no more than 0.02 (6%) for the datum case*.

For installations with z/c of the order 0.34 the effect of removing much of the boundary layer on the jet tube is seen to be small (Fig.19) and it is to be expected that the results obtained are applicable to full-scale, when the wake from the nacelle is even thinner. For the installations closer to the wing, the wake, although thinned by suction, may well be reducing the full effect of the jet flow to some extent.

Jet interference is plotted in Fig.20a for the datum configuration at the full range of Mach numbers tested: 0.6 to 0.74. Whilst this spans the critical Mach number of the isolated wing, velocities on the lower surface everywhere remain well subsonic. In spite of the sharp fall in thrust coefficient and indeed the reduction in thrust with increasing Mach number, and also the corresponding reduction in jet velocity increment, the effect of Mach number is negligible apart from a very small but progressive increase in the maximum suction increment. Since the thrust coefficient is a measure of the resistance to deformation of the jet, this lack of sensitivity again implies that the stiffness or solidity of the jet is not important.

A broadly similar result to that of Fig.20a had been obtained earlier, without boundary layer suction with Wing A mounted on the other side of the jet tube ($\theta = 90^{\circ}$ in Fig.8), when the natural boundary layer was relatively thick. Here however there was less evidence of the secondary suction peak on the rear half of the wing, and the first peak increased significantly at Mach numbers above $M_o = 0.68$, when the flow was locally supersonic.

The effect of varying jet pressure ratio is illustrated in Fig.20b. Jet interference increases practically linearly with the increase in jet pressure from the zero thrust condition $H_j = H_o$ (corresponding to $H_j = 1.39\ p_o$ at Mach 0.7) to at least $H_j = 3\ p_o$, but has jumped sharply by $H_j = 4\ p_o$. This value is in fact well beyond the capabilities of the fan of an engine of this type in the speed range considered here. It is noteworthy that the initial linear increase of jet interference with jet pressure extends, without any discontinuity, from a subsonic jet, through the nozzle choking condition and up to a well developed supersonic jet.

---

*The change in section C_L due to the displacement effect of the nozzle is also relatively small, as the mean pressures on the upper and the lower surfaces are increased by a roughly equal amount.

Fig.21 shows the jet interference measured for the remaining configurations tested. Plugging the central nozzle has virtually no effect on the values of ΔC_p, as mentioned earlier in section 2.4. With the wing at lower incidence (configuration No.6), the shape of the jet interference curve is only changed slightly, though the magnitude of ΔC_p is increased. Moving the nacelle rearwards (configuration No.5) increases the maximum value of ΔC_p, shifts the peak rearwards and apparently broadens it somewhat. On Wing A, as already mentioned, the shape of the ΔC_p curve is generally similar to those obtained on Wing B, but the peak is further forward and the secondary peak is both smaller and further back.

The oscillatory shape of the jet interference curve in Figs.19 and 20 seems to be independent of the Mach number, jet pressure ratio, and vertical spacing between nacelle and wing. It also seems to be independent of the wing incidence, but is changed by moving the nacelle rearward, and by changing from Wing B to Wing A with a notably different basic pressure distribution. At first sight, the characteristic pattern of alternate expansions and contractions observed on the wing might be thought to be related to the cellular pattern of compressions and expansions in the jet itself. This is clearly not so, however, since the cell length in the jet varies markedly with jet pressure ratio (see Fig.6). The jet interference is evidently associated with some feature of the jet not represented by the 'equivalent solid body'. Perhaps the most likely origin for the two suction peaks on the wing could be found in the expansions of the jets at the two nozzles. The streamwise distance between the two nozzles is $3\frac{1}{4}$ inches, whereas the distance between the suction peaks in Figs.19 and 20 is about $2\frac{1}{4}$ inches, so the case for relating the two is not strong; another argument against this explanation is that with the central nozzle plugged, the second suction peak on the wing is only slightly diminished (Fig.21).

Another possible origin for the forward suction peak on the wing might be sought in a waviness or sharp change of curvature of the nacelle shape, though it would be necessary to postulate some mechanism whereby the influence of such a feature could be magnified by an increased jet pressure ratio. Reference to Table 2 shows that in fact the shape is not quite smooth at about x_j = 2.2 inches, which corresponds to the first suction peak at x/c = 0.25. The table of differences would be smooth if the diameter at x_j = 2.28 inches were 1.123 inches rather than 1.122 inches; linearised

theory suggests that a 'wave' of this magnitude would give a peak pressure increment of the order of $\Delta C_p = 0.03$ on a two-dimensional flat plate at transonic speeds. However, there is nothing in the schlieren photographs (Fig.6) to suggest that a significant disturbance is generated around here. Furthermore, the second suction peak on the wing is at a position well downstream of the end of the nozzle, so cannot be accounted for by a similar explanation.

It is intended to extend the experiment when the opportunity arises in the hope of finding a more satisfactory explanation for the origin of the suction peaks.

The fact that the jet interference curve does not change significantly with free-stream Mach number over the range M = 0.6 to 0.74 suggests that no great difference is likely at the higher speeds appropriate to a swept wing design. This may not be true, however, if the flow on the wing is locally supersonic, as indicated by the results obtained on Wing A and reported in Ref.2.

6.4 Jet deflection

Oil flow measurements with the equivalent solid body showed that the pressure field of the wing deflected the boundary layer outwards away from the wing in the region near and ahead of the leading edge, and slightly inwards again near the low pressure region on the wing further downstream. In the same way, the wing field will affect not only the wake but also the annular jet. There is some evidence of this in the measurements of the profile of the edge of the jet at a streamwise position close to that of the wing trailing edge (Fig.22). However, the main conclusion here is that the deflection of the jet due to the wing is relatively small.

7 CONCLUSIONS

Tests have been made with a two-dimensional wing and a blown jet to study the influence of jet thrust on the wing pressure distribution for under-wing podded installations representing engines of large bypass ratio. The size of the nacelle relative to the wing was chosen to be typical of a twin-engined short-range transport design.

The main results and conclusions are listed below:-

(1) Results indicate that for this type of installation, unless the engines are mounted very close to the wing, representation of jet thrust is

unnecessary on wind tunnel models at design Mach numbers except perhaps those specifically intended to study and develop the nacelle and pylon design.

(2) Jet thrust has no measurable affect upon the upper surface pressure distribution.

(3) For the datum configuration, typical of recent aircraft studies, and for jet conditions most representative of full scale, there was a measurable though small jet interference on the wing lower surface. The main effect here was to increase suction over an area between 10% and 40% chord, but there was also a secondary suction increment centred near 65% chord. The pressure increment nowhere exceeded $\Delta C_p = \pm 0.1$ and the maximum change in sectional lift coefficient was only about $\Delta C_L = 0.02$.

(4) There is no indication that jet interference will increase the adverse pressure gradient over the rear part of the lower surface to the point where jet-induced boundary layer separation is likely.

(5) The displacement effect of the jet tube with zero thrust, is for representative installations, at least as large as the jet interference. Suction is reduced over the front part of the wing upper surface and over the rear 70% of the lower surface, and increased only over the front 30% of the lower surface.

(6) For the datum configuration the combined effect of jet thrust and of jet tube displacement at zero thrust is to reduce wing suction everywhere except over the front 30% of the lower surface. Since the wing in isolation has its lower surface suction peak further back at 40% chord, the maximum suction coefficient was not increased by the addition of the nacelle and jet. However, when the nacelle was moved rearward, the suction increments due to the jet thrust and due to the displacement flow were superimposed on the suction peak of the isolated wing, and the total result was to increase the peak suction coefficient on the lower surface from -0.4 to -0.9 at the standard value of jet thrust. The results therefore support the conclusion drawn from earlier tests without jet representation that the nacelle should be kept as far ahead of the wing as possible to minimise interference on the wing.

(7) The effect of plugging the central jet exit was small, and consequently it does not seem to be important to represent the flow characteristics of the central jet accurately in this sort of test.

(8) The jet interference effects measured were only slightly dependent on Mach number, so the results measured for the two-dimensional wing should be substantially representative of the interference to be expected at the higher Mach number appropriate to a swept wing.

(9) Whilst jet interference is increased by increasing jet pressure ratio (and by moving the jet tube closer to the wing), the shape of the interference curve, and in particular the positions on the wing chord at which the primary and secondary suction peaks occur, is effectively unchanged. This shows that the fluctuations in the interference curve are not induced by the recurring expansion and shock waves within the supersonic jet.

(10) Representing the jet by an equivalent solid body, the shape of which corresponds to the outer edge of the jet but with no representation of the expansion of the jet downstream of the nozzle nor the broadening of the jet due to entrainment from the main stream, produces a pressure distribution on the wing similar to that for zero thrust. This indicates that the momentum flow or "solidity" of the jet is not an important factor in determing jet interference, for this type of annular nozzle at least.

(11) No satisfactory explanation has been found for the two suction peaks which make up the main part of the interference curve. It is hoped to make some further investigation into this when the opportunity arises.

Acknowledgements

Mr. J. Osborne of Aerodynamics Division, N.P.L. kindly arranged the loan of the wing models used in this investigation.

Table 1

AEROFOIL ORDINATES

	Wing A NPL 1211		Wing B NPL 3151	
x/c	(z/c) Upper surface	(z/c) Lower surface	(z/c) Upper surface	(z/c) Lower surface
Trailing edge				
1.000000	0.00025	-0.00025	0.000300	-0.000300
0.997592	0.00064	-0.00044	0.000664	-0.000621
0.990393	0.00181	-0.00101	0.001751	-0.001582
0.978470	0.00376	-0.00196	0.003552	-0.003173
0.961940	0.00647	-0.00327	0.006049	-0.005378
0.940961	0.00989	-0.00495	0.009218	-0.008178
0.915735	0.01402	-0.00696	0.013029	-0.011544
0.886505	0.01879	-0.00929	0.017445	-0.015444
0.853553	0.02417	-0.01191	0.022422	-0.019841
0.817197	0.03011	-0.01481	0.027914	-0.024692
0.777785	0.03656	-0.01794	0.033868	-0.029950
0.735698	0.04318	-0.02128	0.040234	-0.035566
0.691342	0.04950	-0.02480	0.046774	-0.041426
0.645142	0.05528	-0.02846	0.053053	-0.047147
0.597545	0.06038	-0.03226	0.058963	-0.052637
0.549009	0.06467	-0.03615	0.064245	-0.057555
0.500000	0.06807	-0.03979	0.068673	-0.061587
0.450991	0.07033	-0.04279	0.071925	-0.064475
0.402455	0.07196	-0.04474	0.073609	-0.065991
0.354858	0.07237	-0.04533	0.073523	-0.065977
0.308658	0.07185	-0.04475	0.071972	-0.064628
0.264302	0.07042	-0.04352	0.069281	-0.062119
0.222215	0.06809	-0.04181	0.065570	-0.058850
0.182803	0.06478	-0.03986	0.060997	-0.054903
0.146447	0.06050	-0.03786	0.055671	-0.050329
0.113495	0.05569	-0.03597	0.049739	-0.045261
0.084265	0.04985	-0.03399	0.043290	-0.039710
0.059039	0.04389	-0.03185	0.036487	-0.033773
0.038060	0.03704	-0.02854	0.029375	-0.027625
0.021530	0.02907	-0.02363	0.022164	-0.021236
0.009607	0.02002	-0.01700	0.014830	-0.014630
0.002408	0.01014	-0.00890	0.007620	-0.007580
0	0	0	0	0
Leading edge				
Leading edge radius	ρ/c = 0.019184		ρ/c = 0.013598	

Table 2

NOZZLE ORDINATES

See also Fig.3

Outer nozzle			Inner nozzle			
x_j	Inside diameter	Outside diameter	x_j	Inside diameter	Outside diameter	Difference
-5.5	1.64	2.49	-3.5	0.89	0.89	-
-4.5	1.70	↓	-3.375	0.80	1.02	
-4.0	1.75		-3.25	↓	1.09	
-3.75	1.79		-3.0		1.21	
-3.5	1.84		-2.75		1.32	
-3.25	1.92		-2.5		1.39	
-3.0	2.00		-2.375		1.40	
-2.75	2.08	↓	-1.0		1.40	
-2.48	2.13	2.492	-0.625		1.54	
-2.28	2.14	2.493	-0.25		1.68	
-2.08	↓	2.490	-0.02		1.6766	
-1.88		2.479	0.08		1.6770	
-1.68		2.464	0.18		1.6762	0.0008
-1.48		2.445	0.28		1.6738	0.0024
-1.28		2.421	0.38		1.6677	0.0061
-1.08		2.391	0.48		1.6573	0.0104
-0.88		2.358	0.58		1.6440	0.0133
-0.68		2.322	0.68		1.6290	0.0150
-0.48		2.285	0.78		1.6122	0.0168
-0.28		2.247	0.88		1.5939	0.0183
-0.08		2.201	0.98		1.5739	0.0200
0	2.14	2.169	1.08		1.5520	0.0219
			1.18		1.5281	0.0239
			1.28		1.5012	0.0269
			1.38		1.4728	0.0284
			1.48		1.4411	0.0317
			1.58		1.4076	0.0335
			1.68		1.372	0.036
			1.78		1.333	0.039
			1.88		1.293	0.040
			1.98		1.251	0.042
			2.08	↓	1.209	0.042
			2.18	0.80	1.166	0.043
			2.28	← linear	1.122	0.044
			2.38		1.079	0.043
			2.48		1.035	0.044
			2.58		0.991	0.044
			2.68		0.947	0.044
			2.78		0.903	0.044
			2.88		0.859	0.044
			2.98		0.815	0.044
			3.08	taper →	0.768	0.047
			3.21	0.73	0.7506	

Note: All dimensions in inches; measurements were made to quoted accuracy.

Table 3

ORDINATES OF EQUIVALENT SOLID BODY

(see Fig.5)

Dimensions in inches	
x_j	Diameter
0.02	2.138
0.22	2.133
0.42	2.119
0.62	2.109
0.82	2.082
1.02	2.047
1.22	2.004
1.42	1.954
1.62	1.898
1.82	1.840
2.02	1.781
2.22	1.723
2.42	1.667
2.62	1.617
2.82	1.573
3.02	1.540
3.22	1.518
3.42	1.510
3.62	1.503
3.82	1.503
Constant to	
8.49	1.503

SYMBOLS

c	wing chord
C_p	pressure coefficient
C_p^*	critical pressure coefficient (for which M = 1)
ΔC_{pJ}	increment in pressure coefficient due to jet thrust
H	stagnation pressure
H_j	stagnation pressure of jet stream
H_o	stagnation pressure of free stream
M	local Mach number
M_o	free stream Mach number
p_o	static pressure in free stream
R_o	external radius of annular nozzle: see Fig.5
R_1	internal radius of annular nozzle: see Fig.7
R_2	radius of central nozzle: see Fig.7
R_c	Reynolds number based on chord
x	streamwise ordinate measured from wing leading edge
x_j	streamwise ordinate measured from origin at annular nozzle position
x_n	streamwise distance of wing leading edge downstream of nozzle position: see Fig.5
y	horizontal ordinate perpendicular to stream, measured from origin at wing centre line
z	vertical ordinate measured from origin on nozzle centre line (except in Table 1)
z_n	height of wing leading edge above nozzle centre line: see Fig.5
α	wing incidence
β	wing inclination: see Fig.5
δ	radial ordinate for boundary layer profiles: see Fig.8
θ	angular measurement round nozzle: see Fig.8

REFERENCES

No.	Author(s)	Title, etc.
1	R.E. Wallace J.R. Monk	A technique for testing aerofoil sections at transonic speed. Journal of Aircraft, 3, 35-40, January/February 1966
2	D.J. Raney A.G. Kurn	Unpublished Mintech Report
3	J.E. Rossiter A.G. Kurn	Wind tunnel measurements of the effect of a jet on the time average and unsteady pressures on the base of a bluff afterbody. A.R.C. CP 903 (1965)
4	A.G. Kurn	A base pressure investigation at transonic speeds on an afterbody containing four sonic nozzles and a cylindrical afterbody containing a central sonic nozzle. R.A.E. Technical Note Aero 2869 (A.R.C. 24932) (1963)
5	H.C. Garner (Ed.)	Subsonic wind tunnel wall corrections. Chapter 6: Wall interference in tunnels with ventilated walls. AGARDograph 109 October 1966
6	D. Küchemann J. Weber	Aerodynamics of propulsion. Section 9-11, McGraw, Hill Book Company (1953)
7	W.C. Swan	A discussion of selected aerodynamic problems on integration of propulsion systems with airframe on transport aircraft. AGARDograph 103, Part 1, p 23-68 October 1965

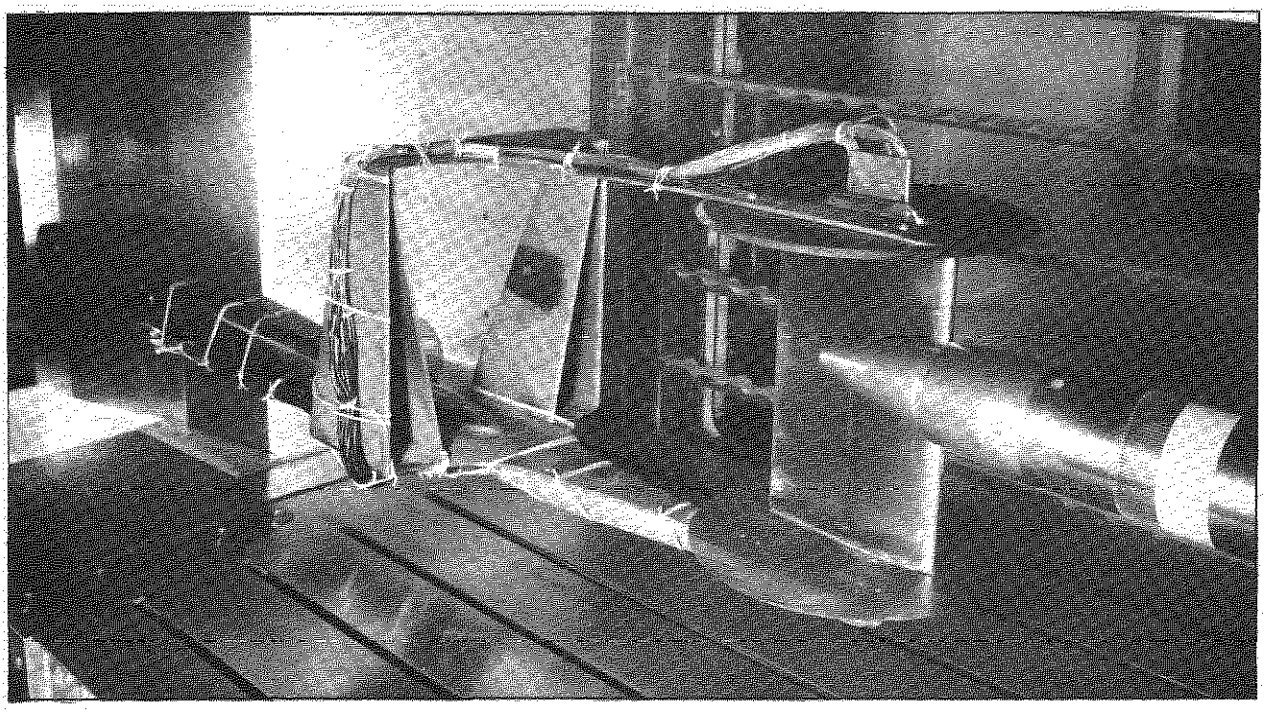

(a)

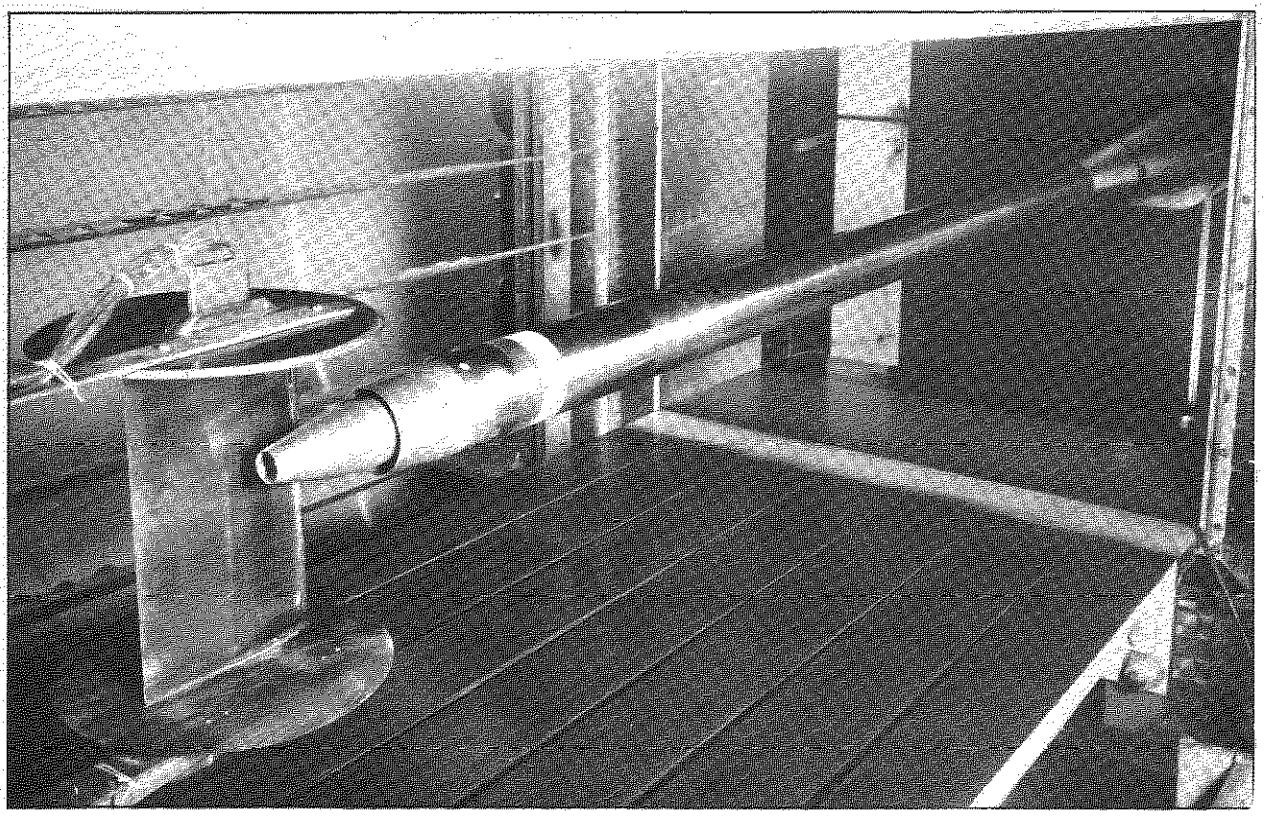

(b)

Fig.1 Model in tunnel

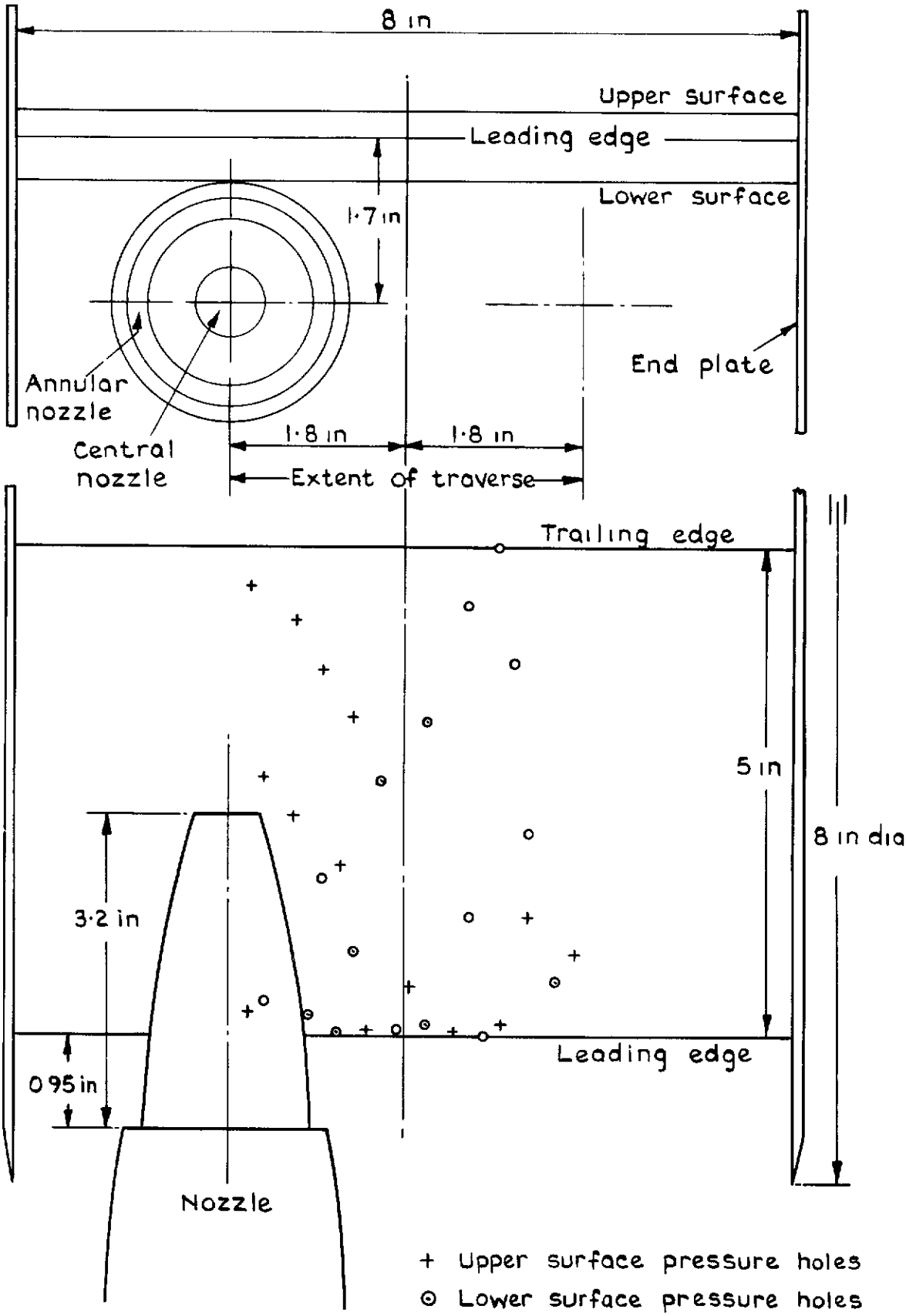

Fig. 2 Model arrangement
Datum configuration

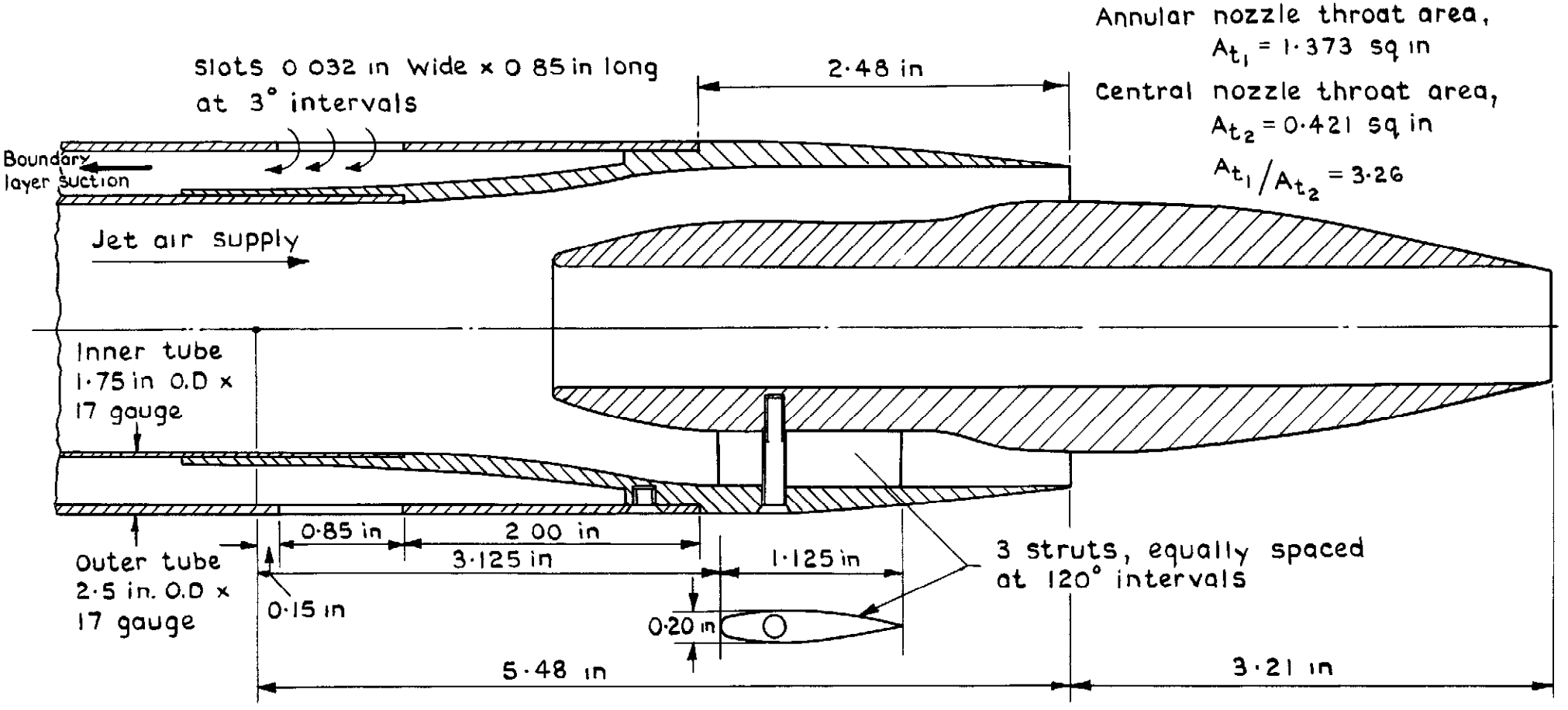

Fig. 3 Nozzle design
See also Table 2

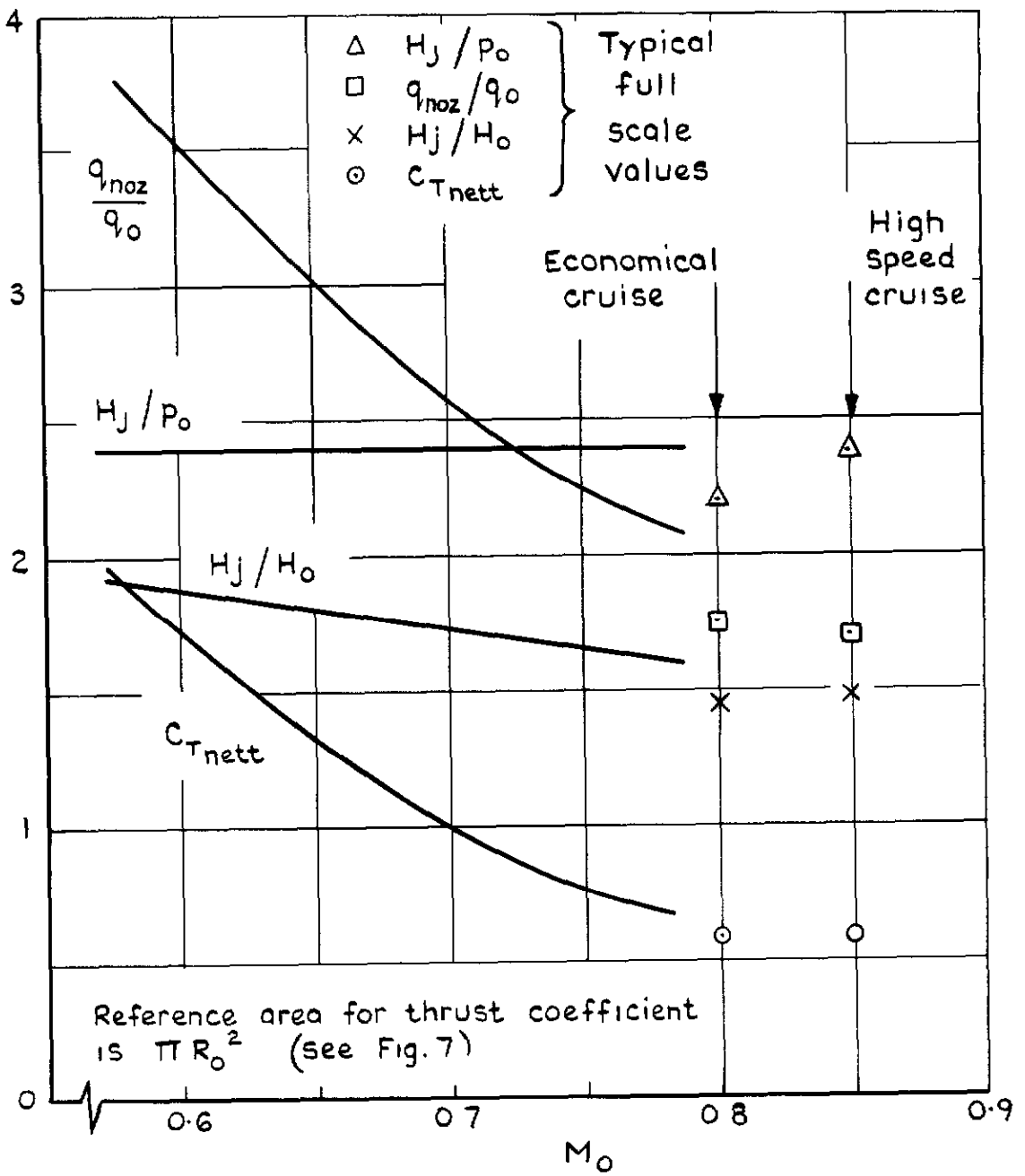

Fig. 4 Variation of jet characteristics with free stream Mach number

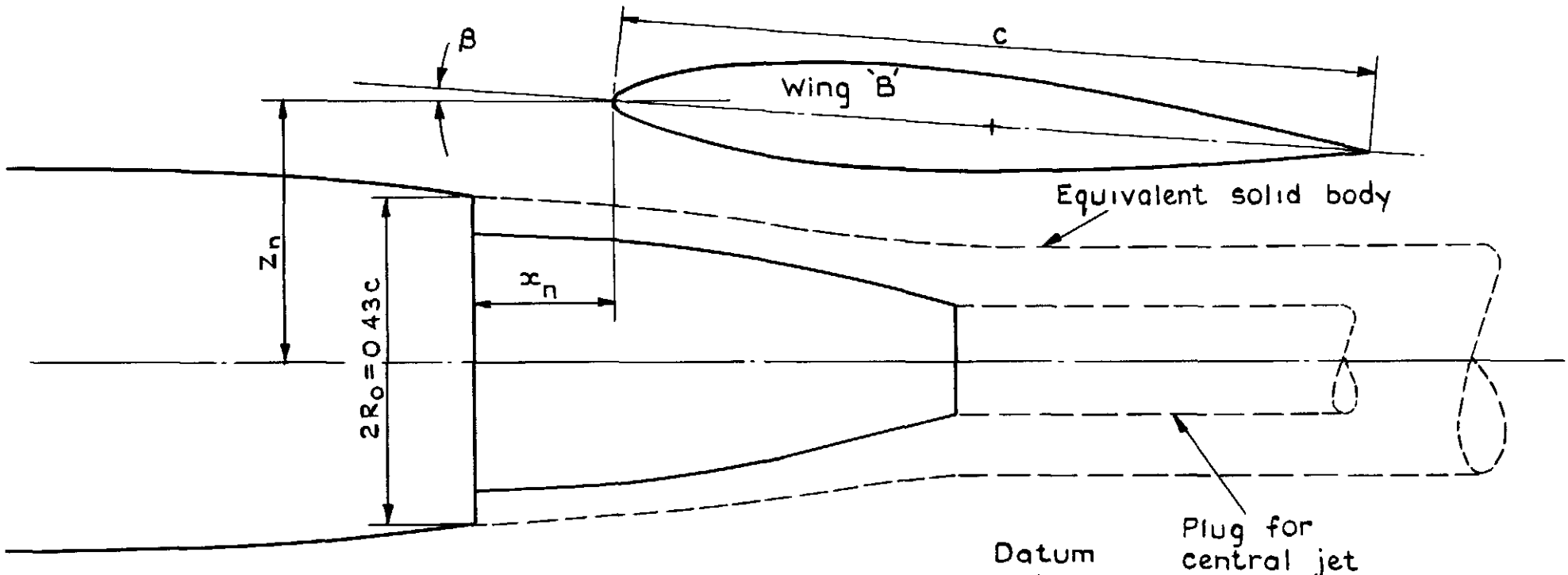

Sketch is of datum configuration
Drawn to scale

Configuration	1	2	3	4	5	6	7
Wing	B	B	B	B	B	B	A
β (deg)	4	4	4	4	4	17	2·1
x_n/c	0·19	0·19	0·19	0·19	−0·06	0·18	0·18
z_n/c	0·38	0·34	0·31	0·28	0·34	0·34	0·34

Fig. 5 Nozzle positions relative to wings

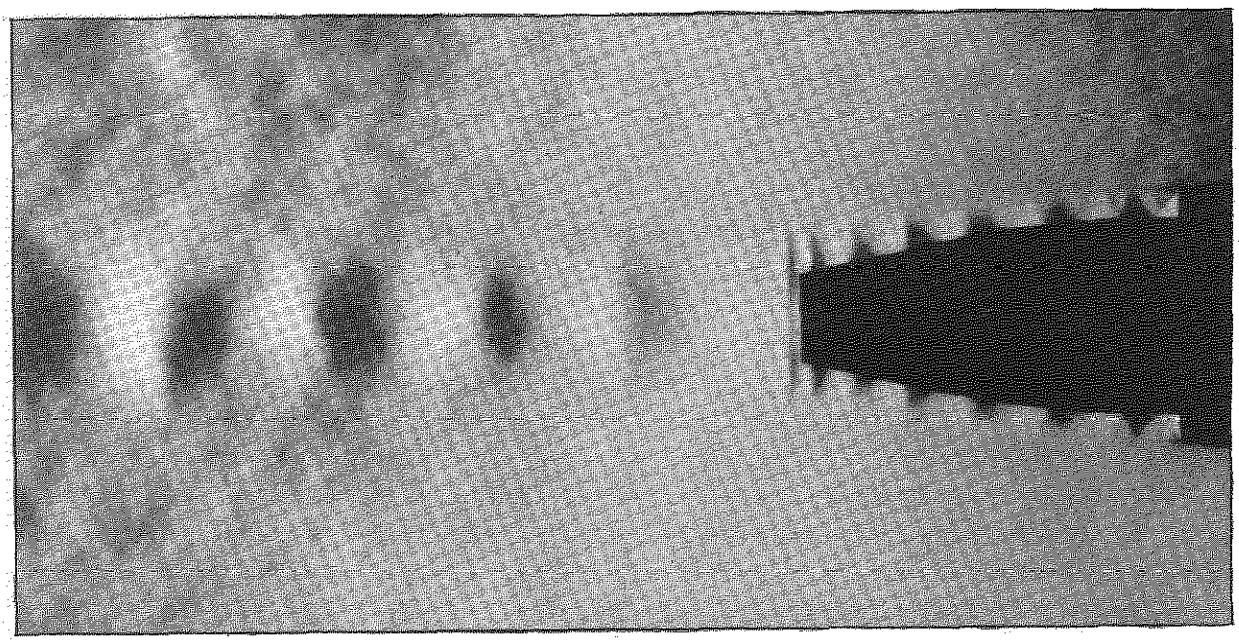

(a) Mo = 0·7 Hj/po = 2·4

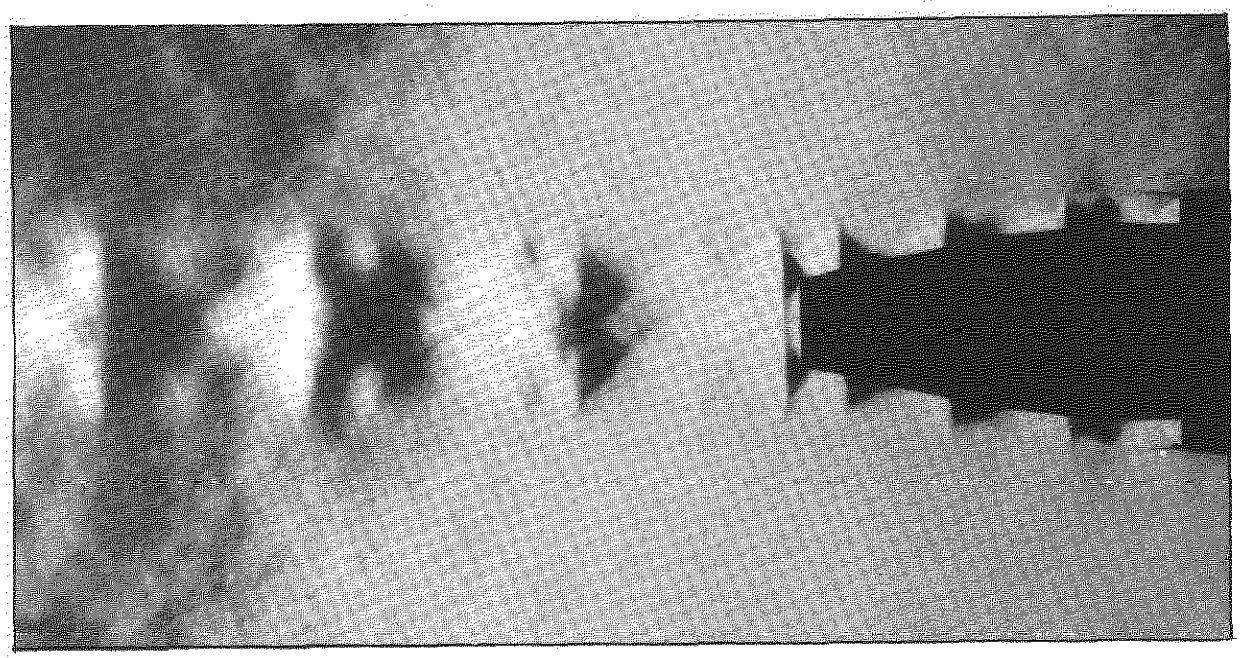

(b) Mo = 0·7 Hj/po = 3·0

Fig.6 Schlieren photographs of flow from bypass nozzle

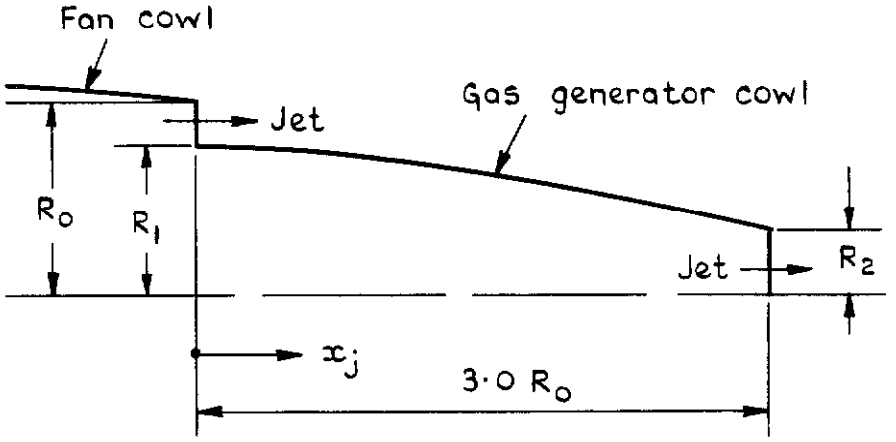

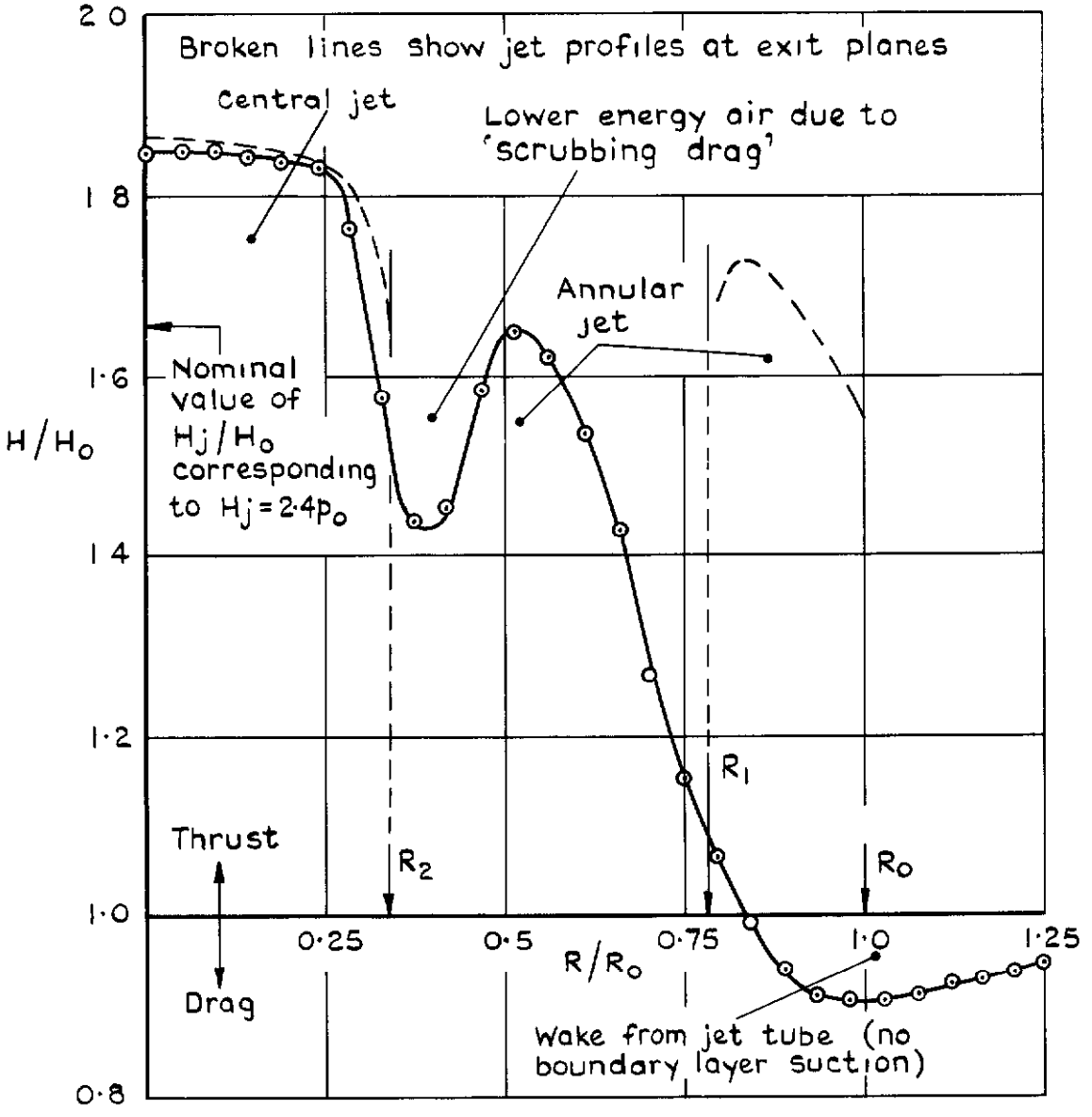

Fig. 7 Jet total head distribution
$H_j = 2{\cdot}4p_0$, $M_0 = 0{\cdot}74$, $x_j = 5{\cdot}6R_0$

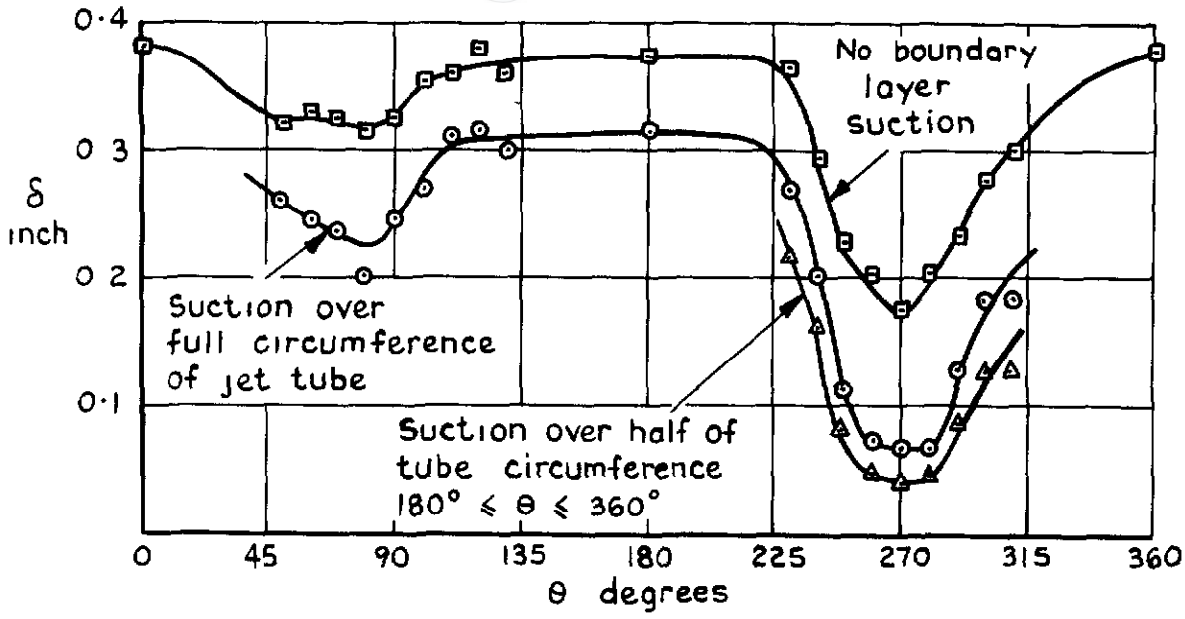

a Boundary layer contour $H/H_o = 0 \cdot 95$

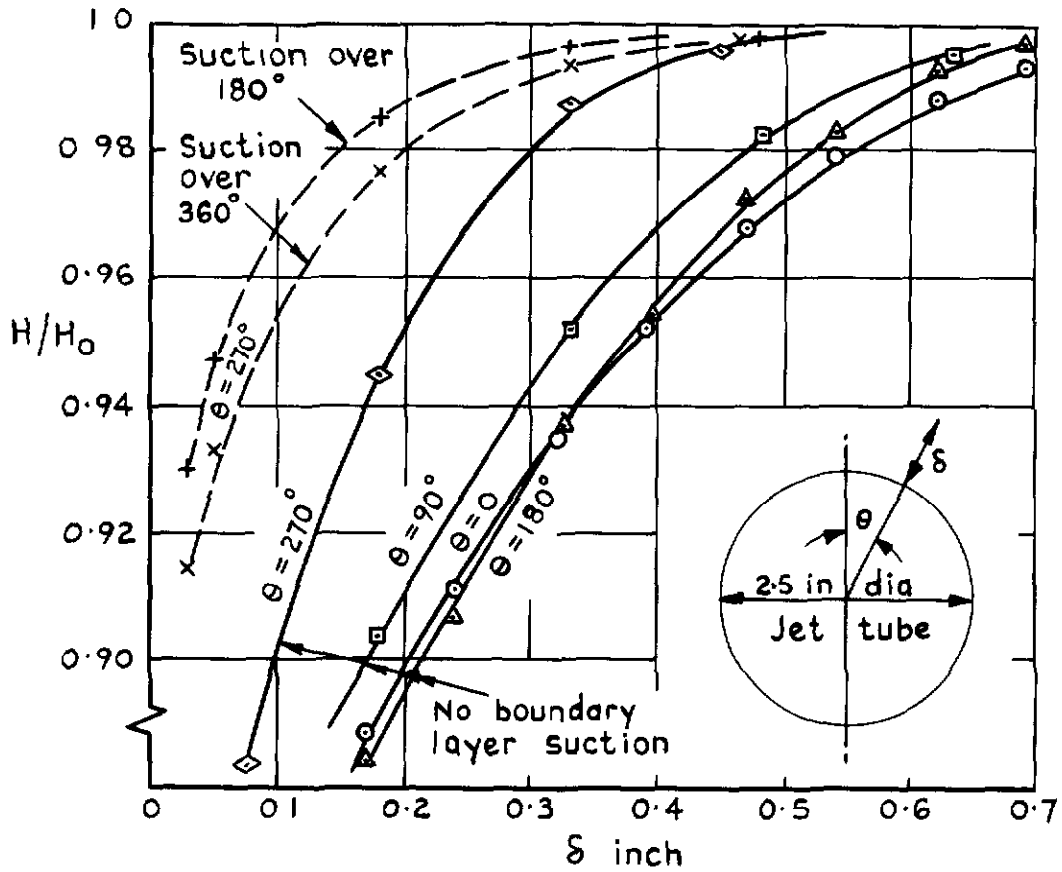

b Boundary layer profiles

Fig. 8a & b Jet tube boundary layer upstream of nacelle shaping $x_j/R_o = -3$, $M_o = 0 \cdot 74$

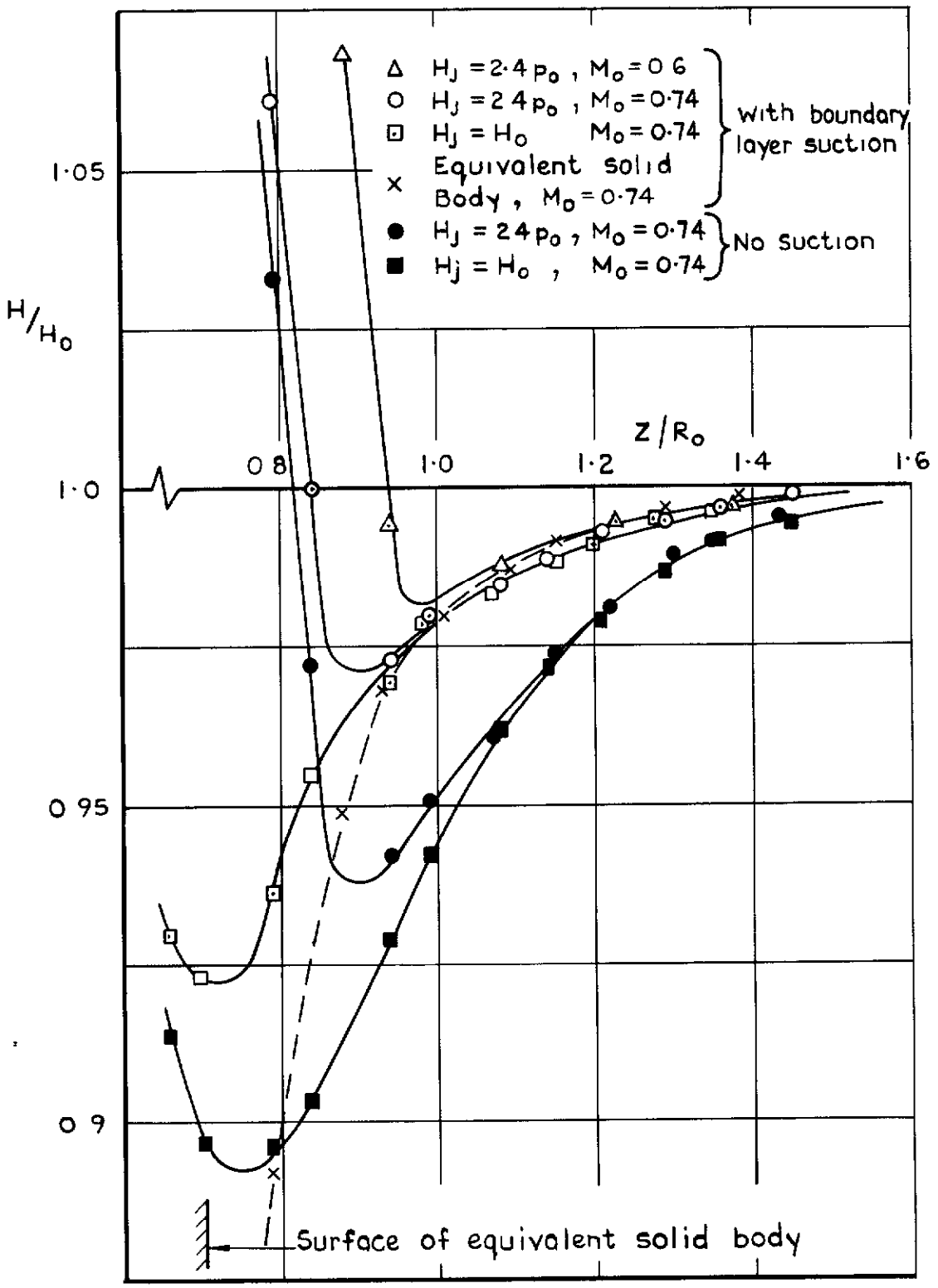

Fig. 9 Jet tube wake profiles $x_J / R_0 = 5{\cdot}6$

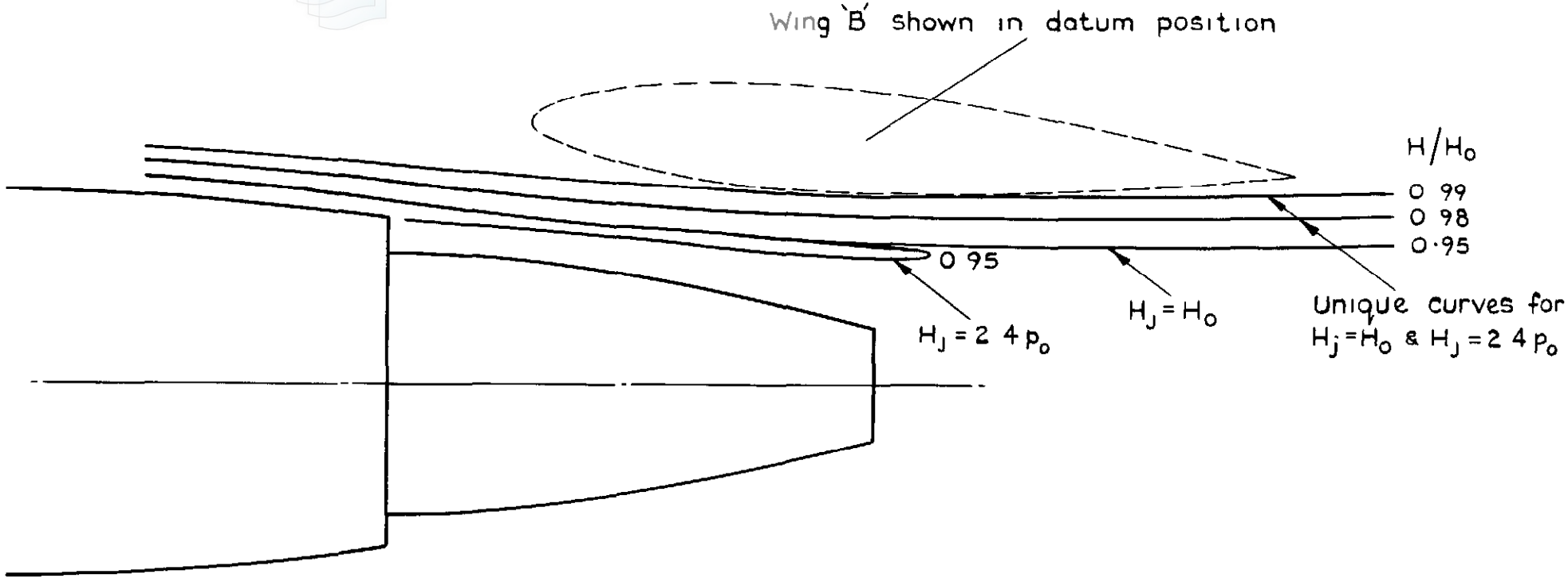

Fig. 10 Total head contours in wake from jet tube.
$M_o = 0{\cdot}74$, boundary layer suction applied, wing not installed

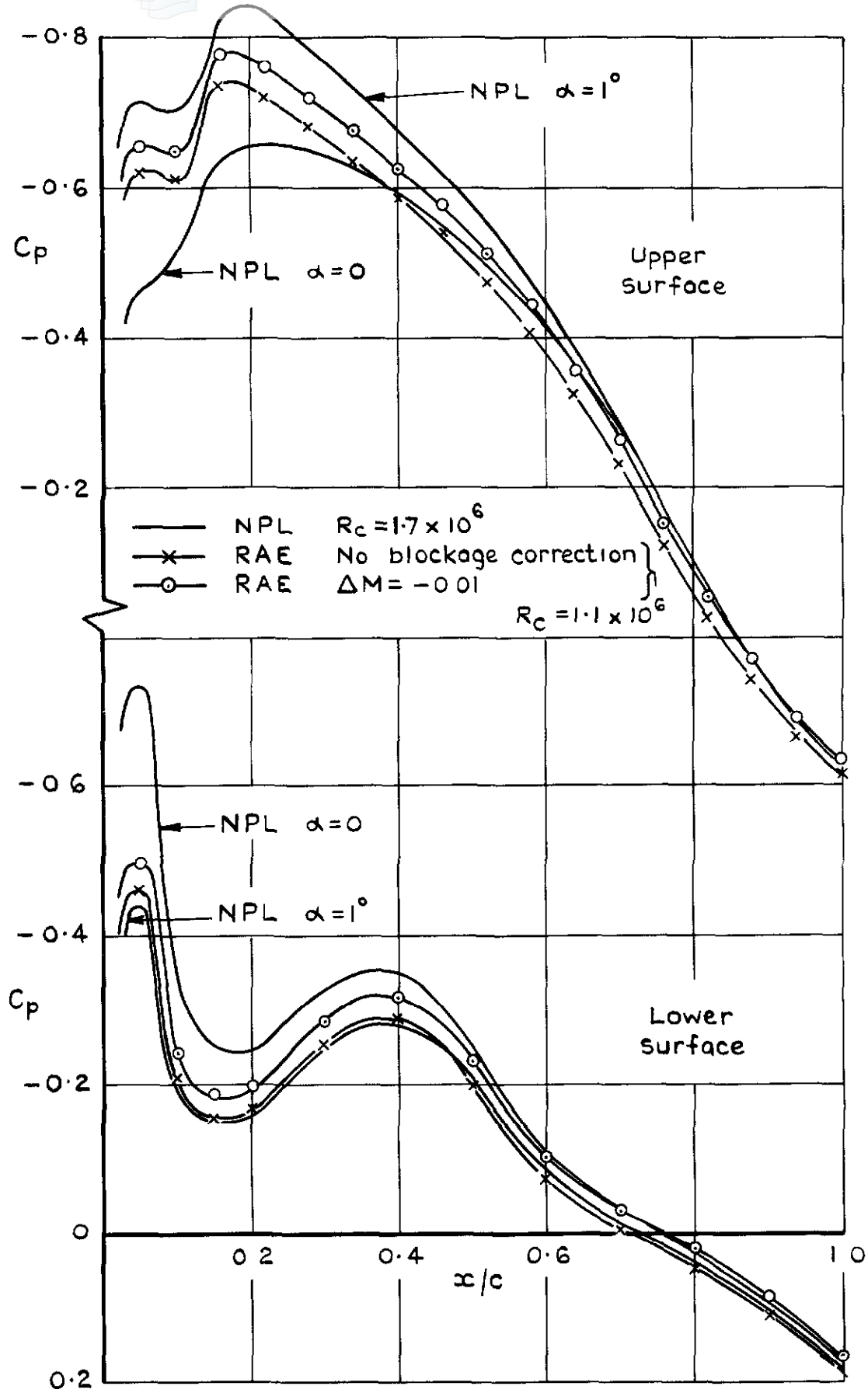

Fig.11 Pressure distribution on Wing A.
Comparison with NPL results, $M_0 = 0{\cdot}72$

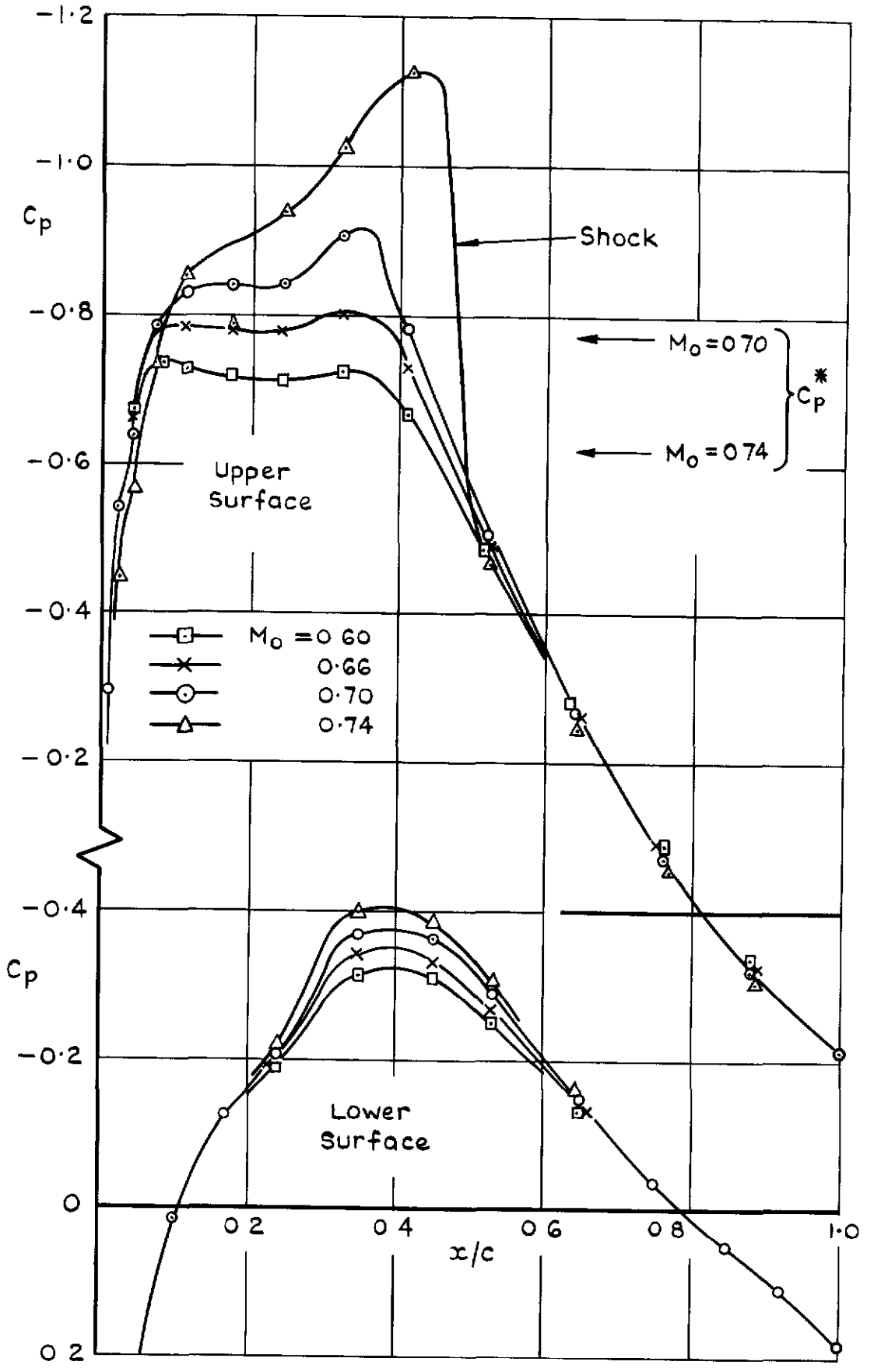

Fig 12 Pressure distribution of Wing B in isolation

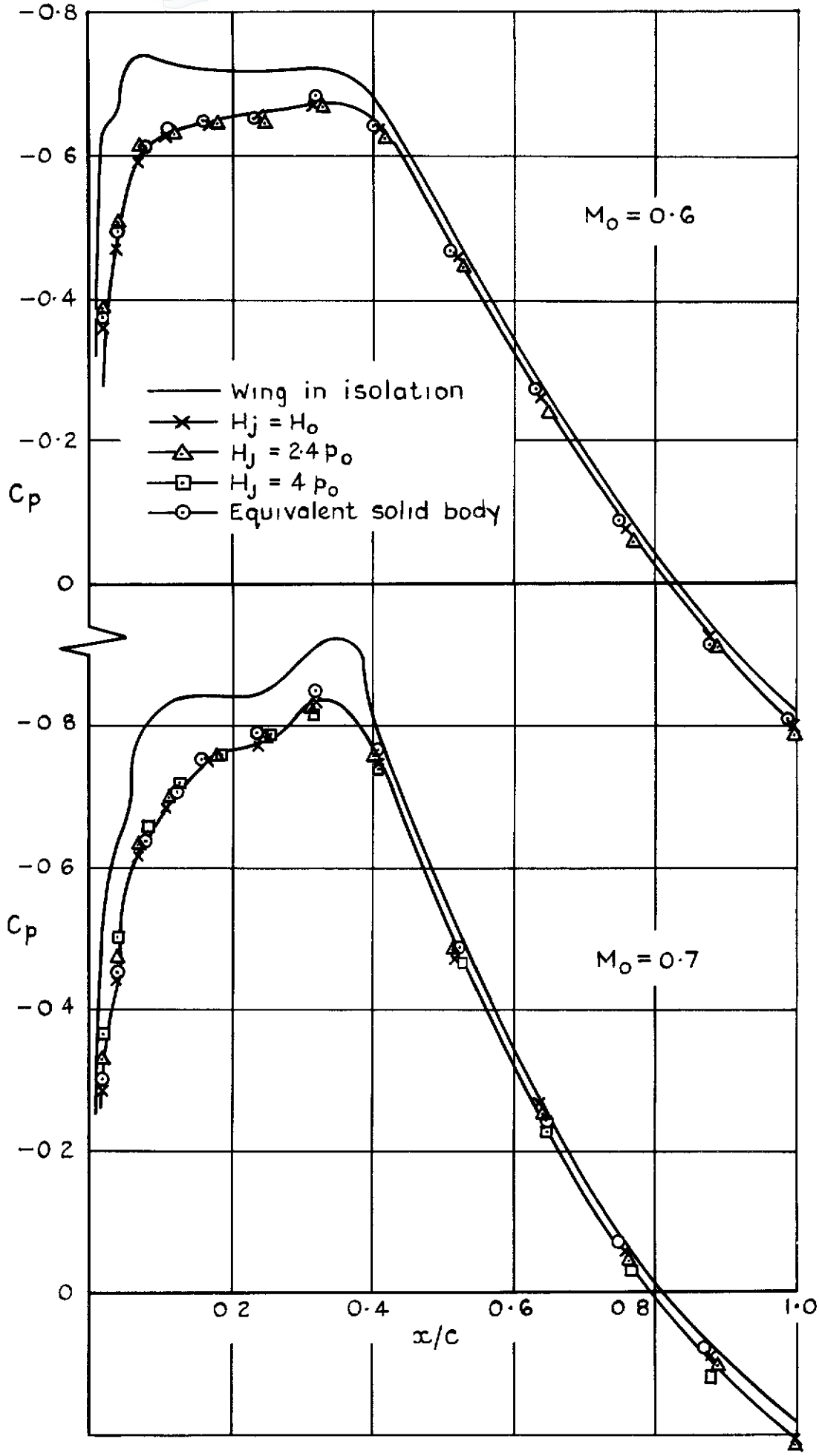

Fig. 13 Upper surface pressures in plane of jet
Datum configuration

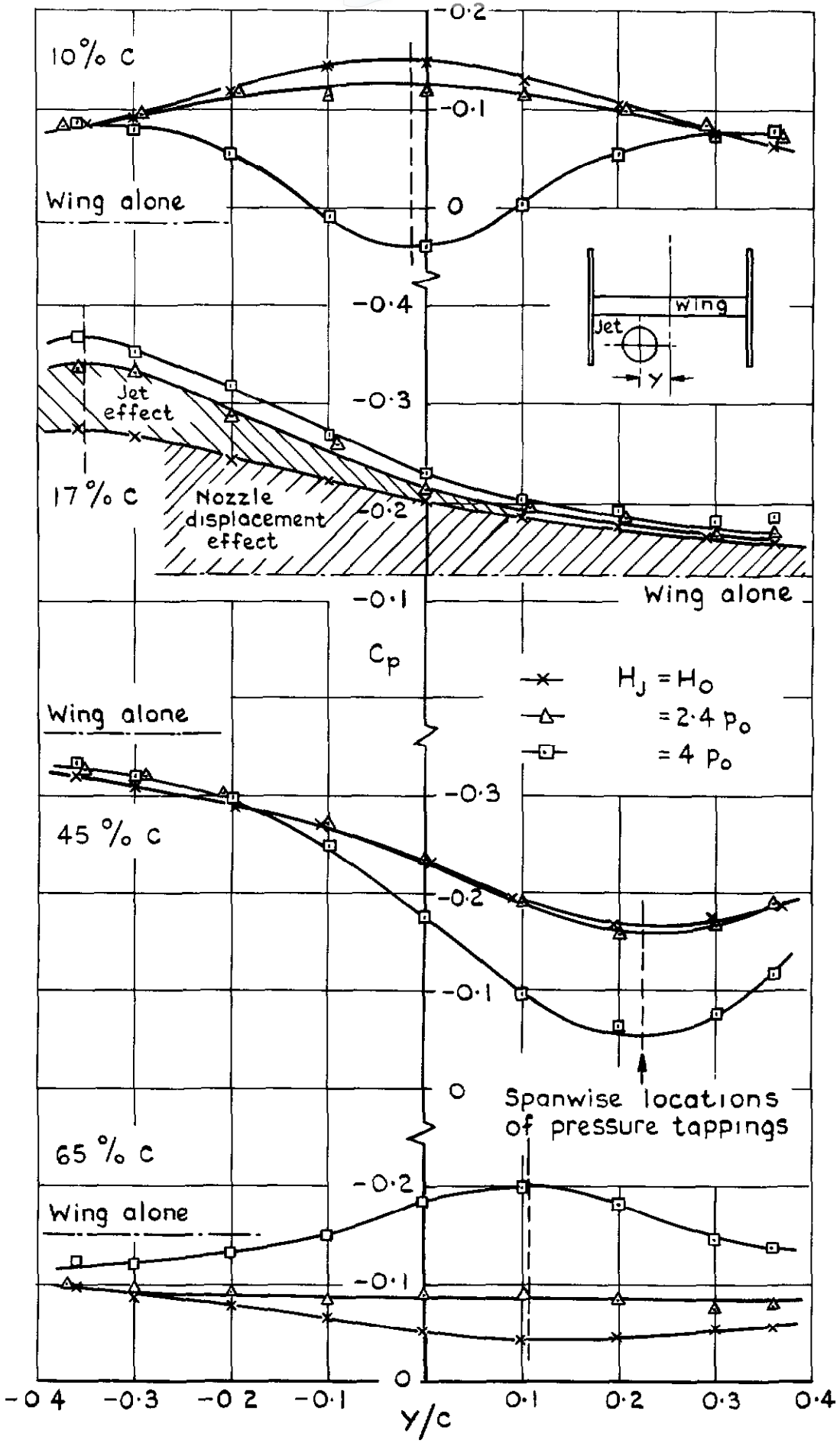

Wing lower surface, datum configuration, $M_o = 0{\cdot}7$

Fig. 14 Typical pressure variations from traverse

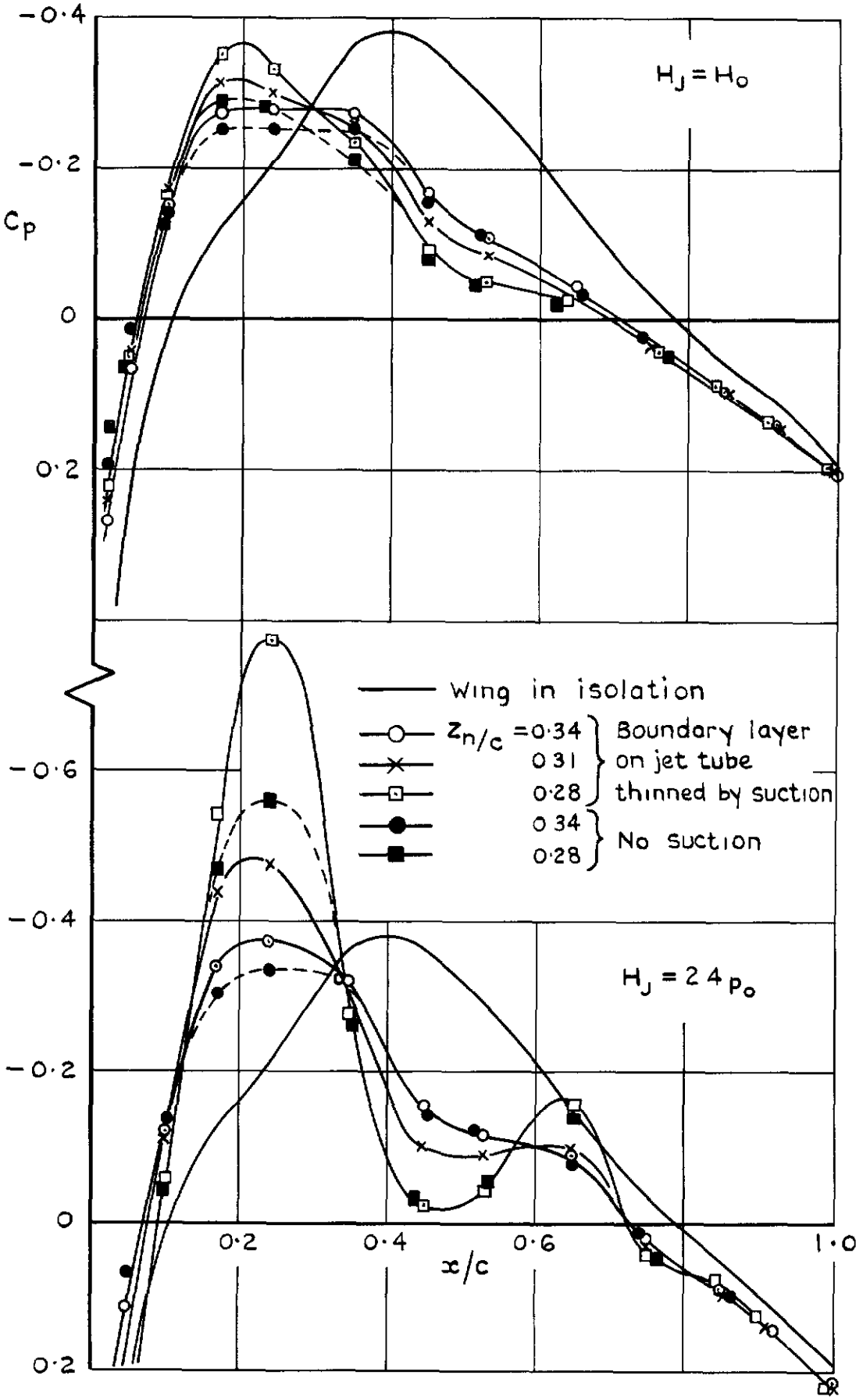

Fig. 15 Effect of jet/wing separation on lower surface pressures in plane of jet, $M_o = 0·7$

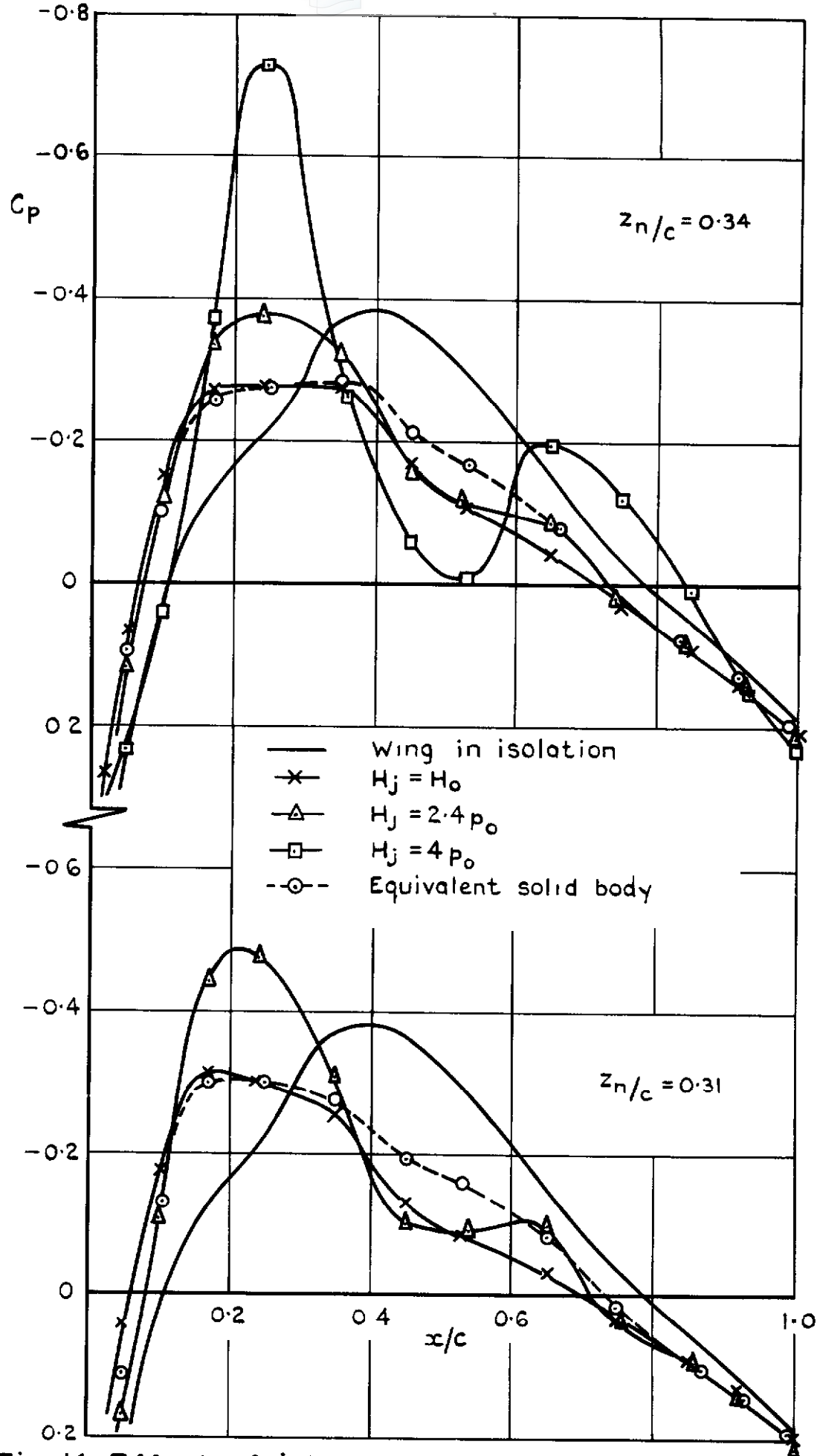

Fig. 16 Effect of jet pressure ratio on lower surface pressures in plane of jet, $M_o = 0·7$

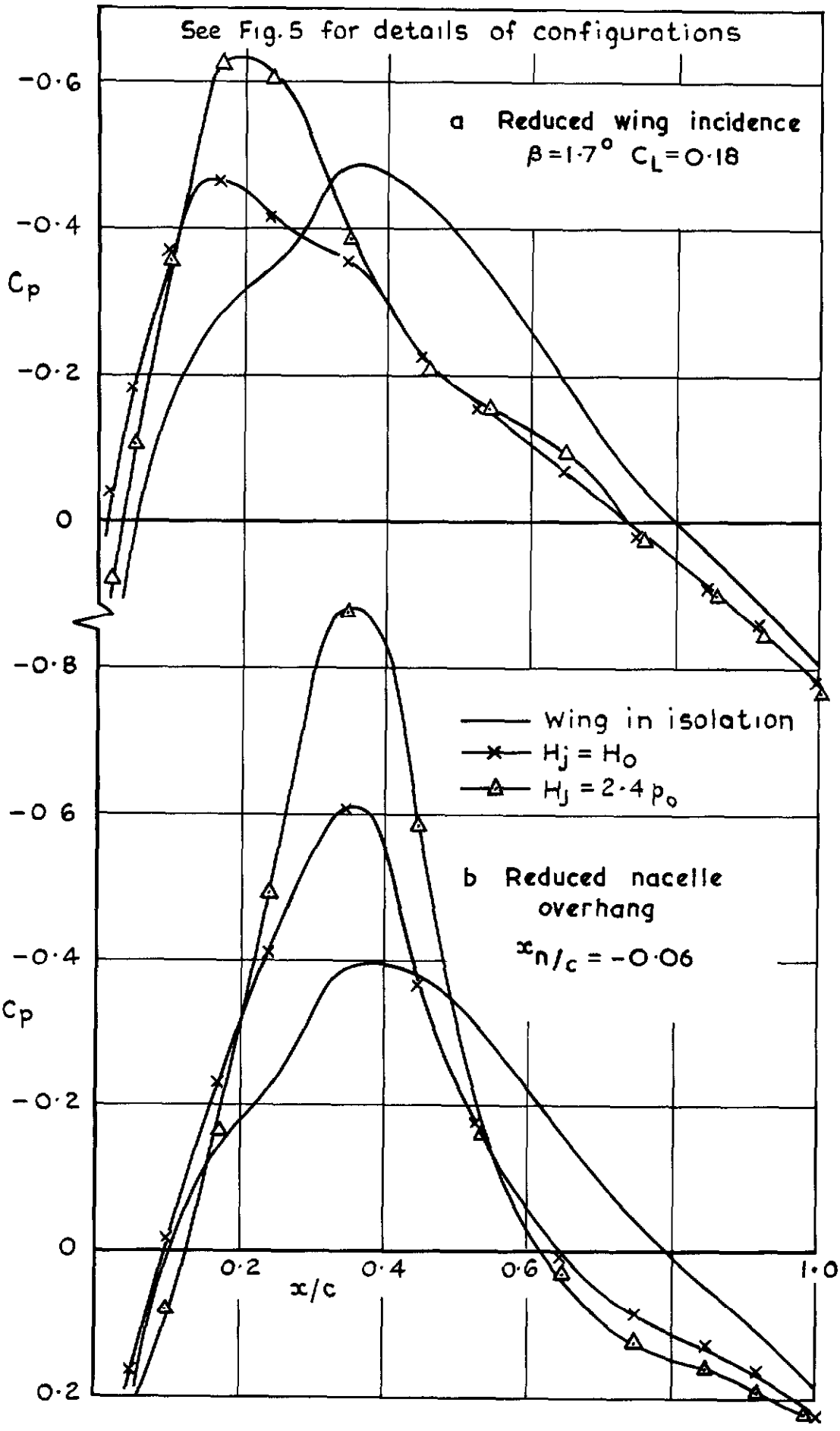

Fig. 17a & b Lower surface pressures in plane of jet for alternative nacelle locations, $M_o = 0{\cdot}7$, $z_{n/c} = 0{\cdot}34$

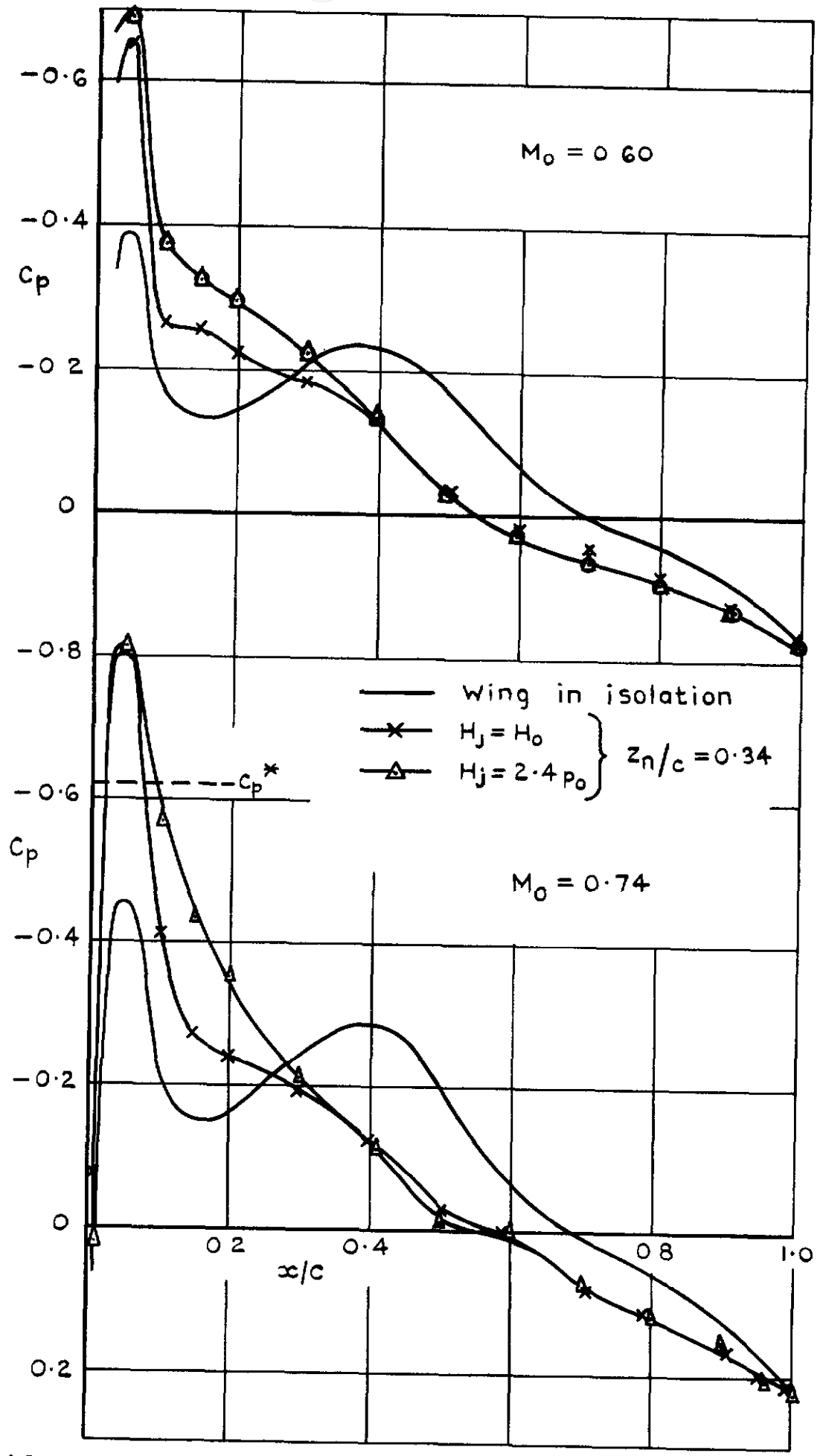

Fig. 18 Lower surface pressures in plane of jet. Wing A
$M_0 = 0{\cdot}6$ & $0{\cdot}74$

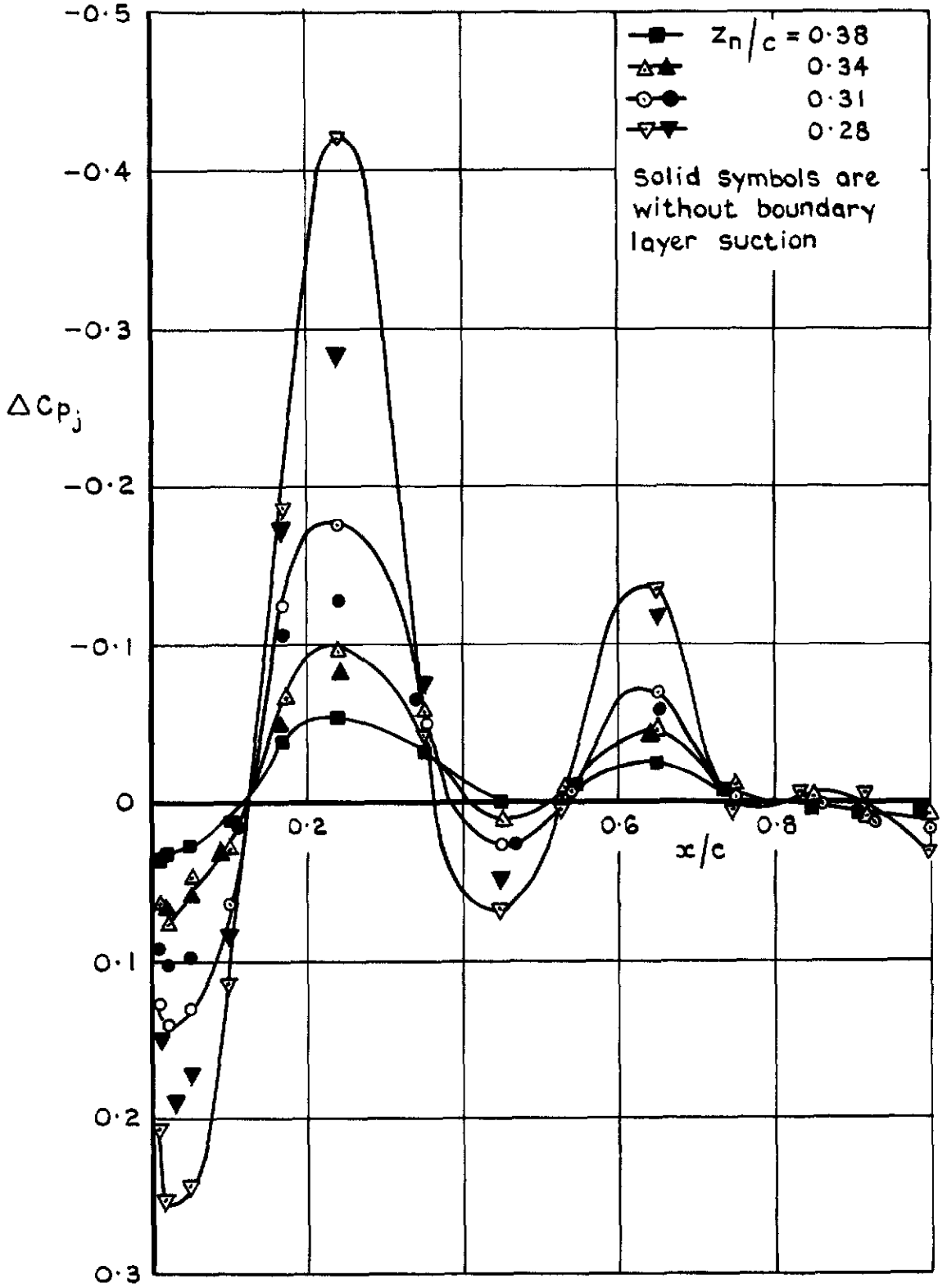

Fig. 19 Effect of jet/wing separation on lower surface pressure increment due to jet blowing. $H_j = 2{\cdot}4p_o$, $M_o = 0{\cdot}7$

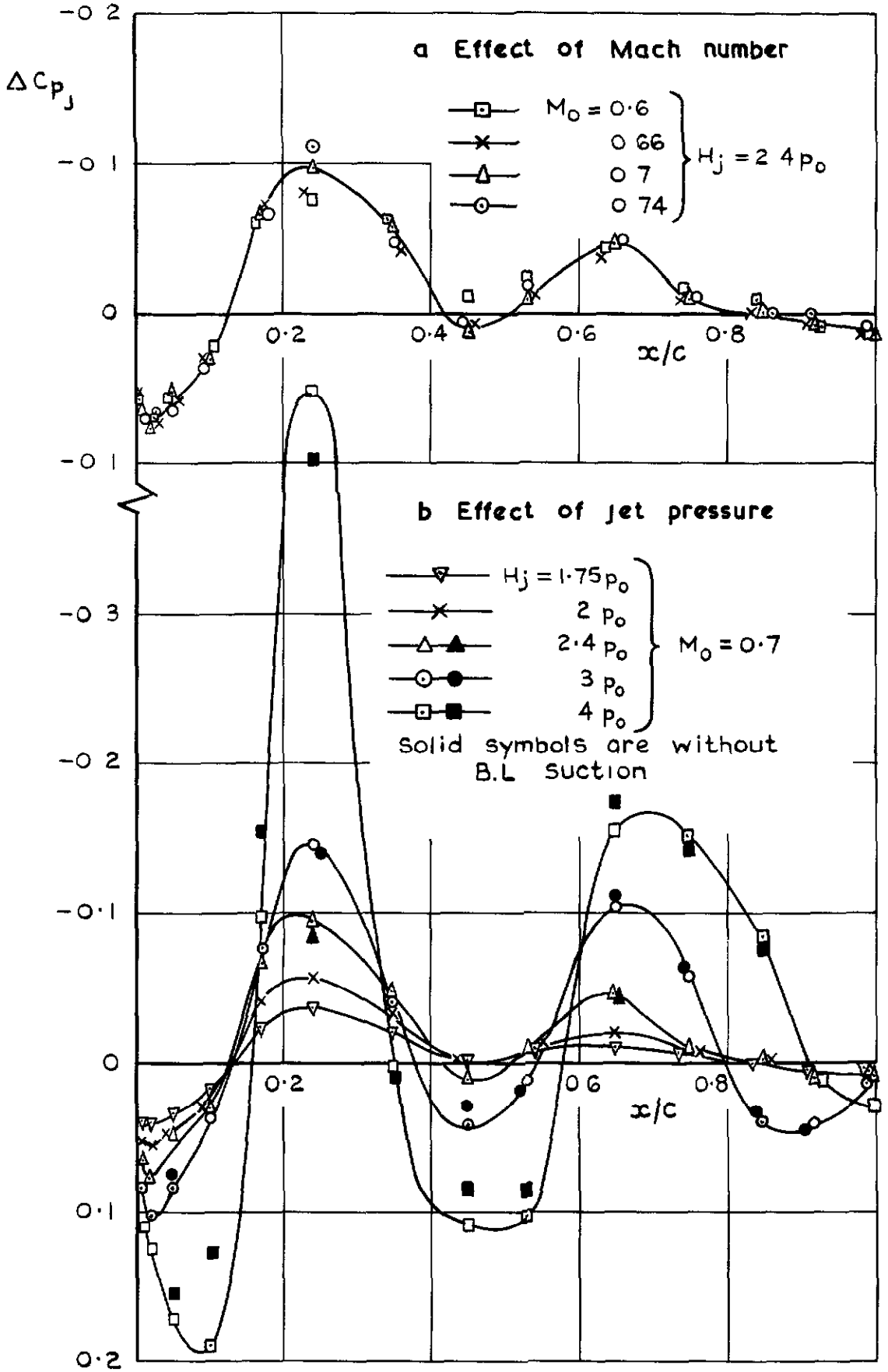

Fig. 20a & b Lower surface pressure increment in plane of jet, due to jet blowing

Datum wing/nacelle configuration

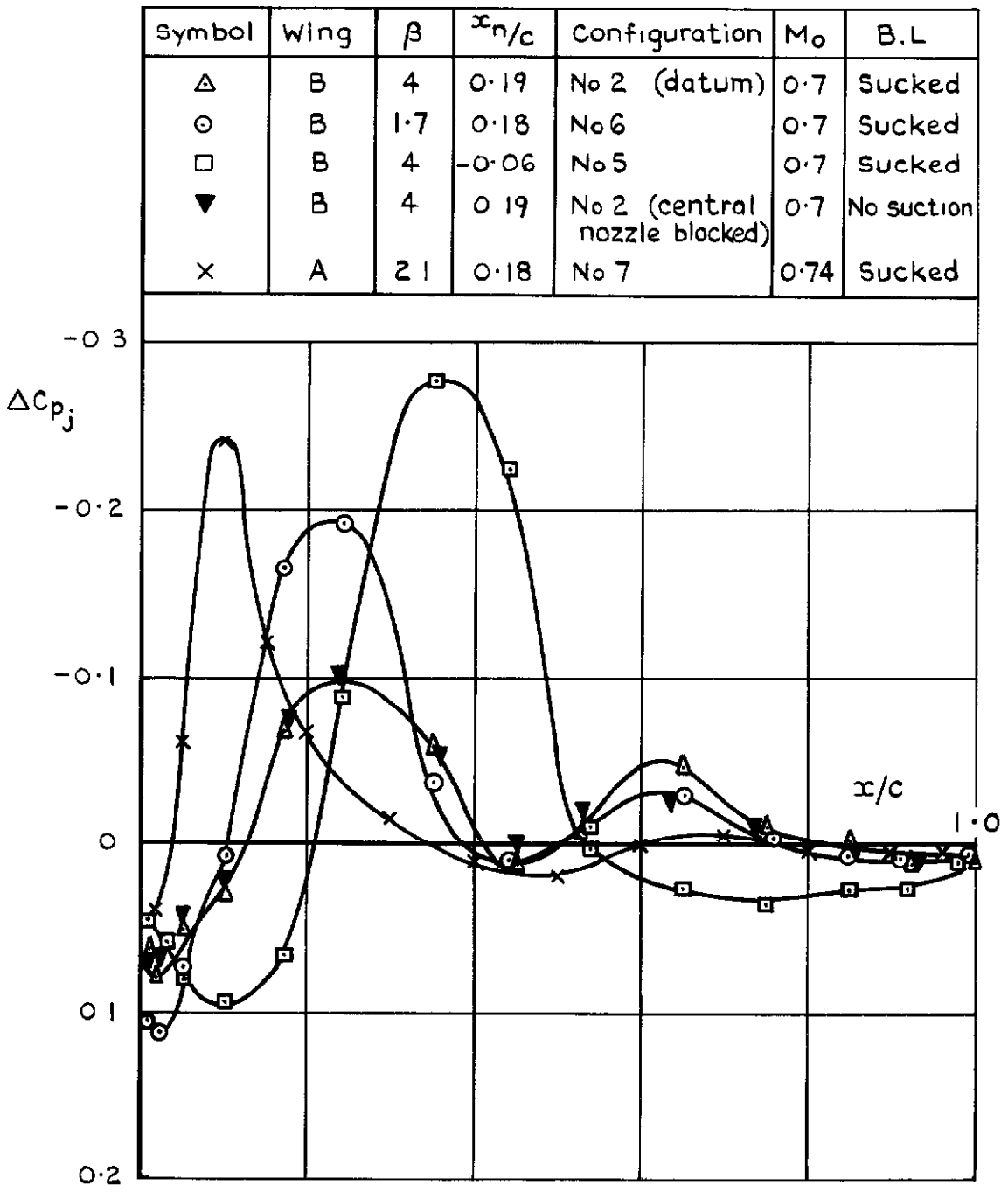

Fig. 21 Lower surface pressure increment in plane of jet due to jet blowing for various jet/wing configurations

Constant vertical separation between jet and wing, $z_n/c = 0.34$

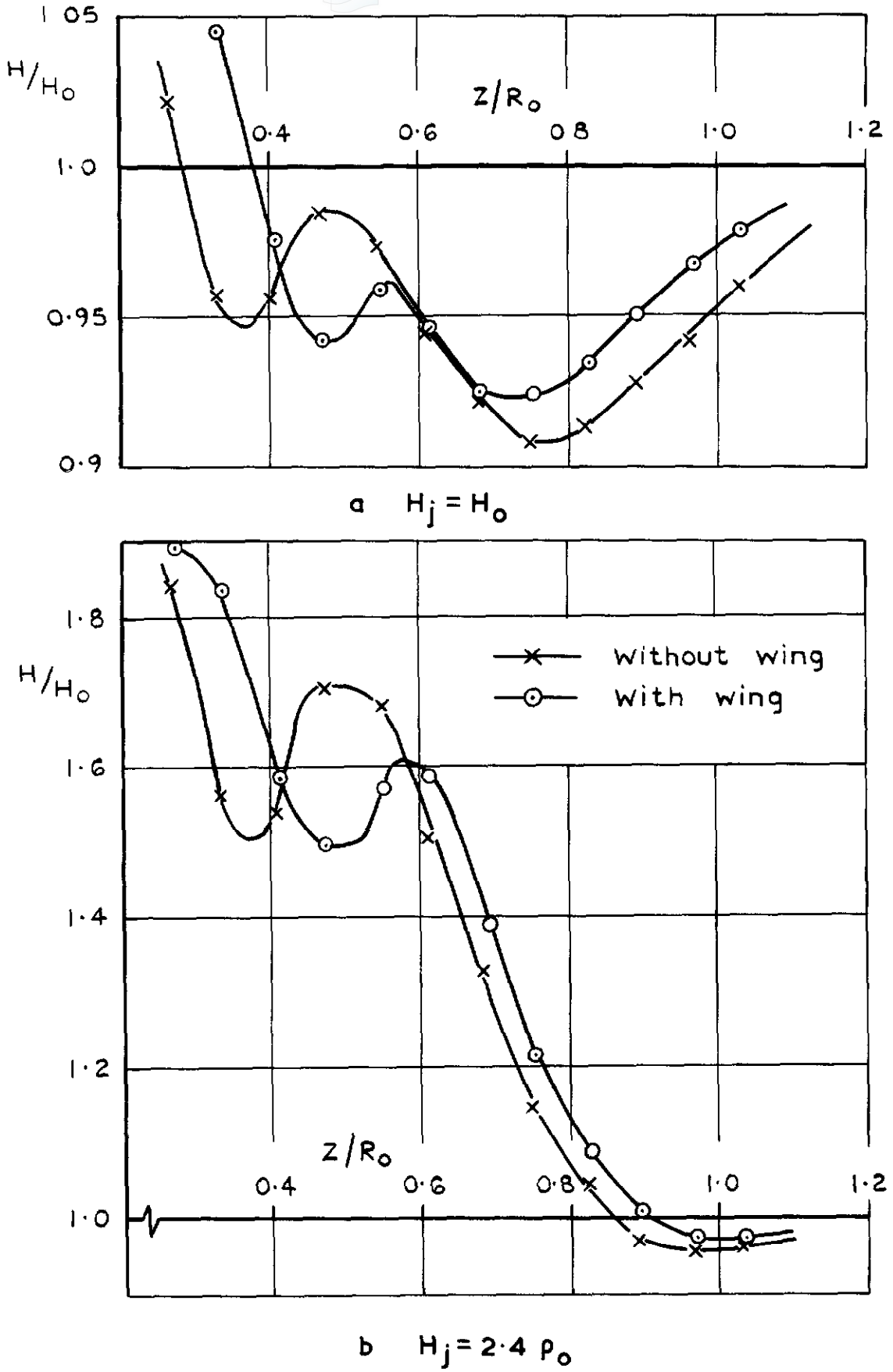

Fig 22a&b Effect of wing on jet total head distribution. Datum configuration, $x_j = 5{\cdot}6\ R_0, M_0 = 0{\cdot}7$

Printed in England for Her Majesty's Stationery Office by the Royal Aircraft Establishment, Farnborough. Dd.135645. K.3.

A.R.C. C.P. No. 1044
March 1968

533.695.178 :
533.6.08 :
533.6.048.2 :
533.6.071

Raney, D.J., Kurn, A.G.,
Bagley, J.A.

WIND TUNNEL INVESTIGATION OF JET INTERFERENCE FOR UNDERWING INSTALLATION OF HIGH BYPASS RATIO ENGINES

Current design proposals for many swept-winged aircraft have large engines of high bypass ratio with short fan cowls on short pylons under the wing, with the annular fan nozzle close to the wing leading edge. With such an arrangement there may be significant changes in the wing pressure distribution induced by the jet flow, particularly that from the fan. In consequence, the normal method of simulating the engine flow in a wind tunnel model, by using simple open ducts, and no representation of the jet thrust, might not be adequate.

The tests reported here were planned as an initial investigation of jet interference for this type of configuration. Results show that for

(over)

A.R.C. C.P. No. 1044
March 1968

533.695.178 :
533.6.08 :
533.6.048.2 :
533.6.071

Raney, D.J., Kurn, A.G.,
Bagley, J.A.

WIND TUNNEL INVESTIGATION OF JET INTERFERENCE FOR UNDERWING INSTALLATION OF HIGH BYPASS RATIO ENGINES

Current design proposals for many swept-winged aircraft have large engines of high bypass ratio with short fan cowls on short pylons under the wing, with the annular fan nozzle close to the wing leading edge. With such an arrangement there may be significant changes in the wing pressure distribution induced by the jet flow, particularly that from the fan. In consequence, the normal method of simulating the engine flow in a wind tunnel model, by using simple open ducts, and no representation of the jet thrust, might not be adequate.

The tests reported here were planned as an initial investigation of jet interference for this type of configuration. Results show that for

(over)

A.R.C. C.P. No. 1044
March 1968

533.695.178 :
533.6.08 :
533.6.048.2 :
533.6.071

Raney, D.J., Kurn, A.G.,
Bagley, J.A.

WIND TUNNEL INVESTIGATION OF JET INTERFERENCE FOR UNDERWING INSTALLATION OF HIGH BYPASS RATIO ENGINES

Current design proposals for many swept-winged aircraft have large engines of high bypass ratio with short fan cowls on short pylons under the wing, with the annular fan nozzle close to the wing leading edge. With such an arrangement there may be significant changes in the wing pressure distribution induced by the jet flow, particularly that from the fan. In consequence, the normal method of simulating the engine flow in a wind tunnel model, by using simple open ducts, and no representation of the jet thrust, might not be adequate.

The tests reported here were planned as an initial investigation of jet interference for this type of configuration. Results show that for

(over)

A.R.C. C.P. No. 1044
March 1968

533.695.178 :
533.6.08 :
533.6.048.2 :
533.6.071

Raney, D.J., Kurn, A.G.,
Bagley, J.A.

WIND TUNNEL INVESTIGATION OF JET INTERFERENCE FOR UNDERWING INSTALLATION OF HIGH BYPASS RATIO ENGINES

Current design proposals for many swept-winged aircraft have large engines of high bypass ratio with short fan cowls on short pylons under the wing, with the annular fan nozzle close to the wing leading edge. With such an arrangement there may be significant changes in the wing pressure distribution induced by the jet flow, particularly that from the fan. In consequence, the normal method of simulating the engine flow in a wind tunnel model, by using simple open ducts, and no representation of the jet thrust, might not be adequate.

The tests reported here were planned as an initial investigation of jet interference for this type of configuration. Results show that for

(over)

DETACHABLE ABSTRACT CARDS

conventional locations of the nacelle on the wing, representation of the cruising jet thrust has only a small effect upon the wing pressure distribution and then only on the lower surface.

conventional locations of the nacelle on the wing, representation of the cruising jet thrust has only a small effect upon the wing pressure distribution and then only on the lower surface.

conventional locations of the nacelle on the wing, representation of the cruising jet thrust has only a small effect upon the wing pressure distribution and then only on the lower surface.

conventional locations of the nacelle on the wing, representation of the cruising jet thrust has only a small effect upon the wing pressure distribution and then only on the lower surface.

Published by
HER MAJESTY'S STATIONERY OFFICE

To be purchased from
49 High Holborn, London W C.1
13A Castle Street, Edinburgh 2
109 St Mary Street, Cardiff CF1 1JW
Brazennose Street, Manchester 2
50 Fairfax Street, Bristol BS1 3DE
258 Broad Street, Birmingham 1
7 Linenhall Street, Belfast BT2 8AY
or through any bookseller

C.P. No. 1044

SBN 11 470171 7